

---

# Neural Lyapunov Model Predictive Control

---

Mayank Mittal<sup>\*12</sup> Marco Gallieri<sup>\*1</sup> Alessio Quaglino<sup>1</sup> Seyed Sina Mirrazavi Salehian<sup>1</sup> Jan Koutník<sup>1</sup>

## Abstract

This paper presents *Neural Lyapunov MPC*, an algorithm to alternately train a Lyapunov neural network and a stabilising constrained Model Predictive Controller (MPC), given a neural network model of the system dynamics. This extends recent works on Lyapunov networks to be able to train solely from expert demonstrations of one-step transitions. The learned Lyapunov network is used as the value function for the MPC in order to guarantee stability and extend the stable region. Formal results are presented on the existence of a set of MPC parameters, such as discount factors, that guarantees stability with a horizon as short as one. Robustness margins are also discussed and existing performance bounds on value function MPC are extended to the case of imperfect models. The approach is tested on unstable non-linear continuous control tasks with hard constraints. Results demonstrate that, when a neural network trained on short sequences is used for predictions, a one-step horizon Neural Lyapunov MPC can successfully reproduce the expert behaviour and significantly outperform longer horizon MPCs.

## 1. Introduction

Control systems comprise of constraints that need to be considered during the controller designing process. In most robotic applications, these constraints appear as actuator saturations or state boundaries. Typically, a control strategy that violates these specifications can adversely affect the performance of the overall system and lead to *unsafe* behaviors. In this work, we wish to learn robust control policies that can perform set-point reaching tasks safely, i.e., while respecting the constraints in the system.

A pivotal concept to safe control of a dynamics system is the stability of an equilibrium point. One way to verify that a given feedback controller stabilizes a system is by

using Lyapunov functions. If the closed-loop response to a given state maps to a strictly smaller value of the Lyapunov function, then it can be shown that the resulting trajectory eventually converges to the equilibrium point. However, finding an appropriate Lyapunov function is cumbersome. Recently, Berkenkamp et al. (2017) and follow-up works proposed methods that try to learn the Lyapunov function by exploiting the expressive power of neural networks (NNs). These approaches show that the learned Lyapunov NN can be used to produce stability (safety) certificates (Bobiti, 2017; Bobiti & Lazar, 2016) as well as improve an existing controller (Gallieri et al., 2019; Chang et al., 2019).

**Summary of contributions** In this paper, we present *Neural Lyapunov MPC*, an algorithmic framework that obtains a single-step horizon Model Predictive Controller (MPC) for Lyapunov-based control of a non-linear deterministic system with constraints. We justify the choice of a unitary horizon by using an imperfect forward model for predictions. In our proposed framework, alternate learning is used to train a Lyapunov NN in a supervised manner and to tune the parameters of the MPC. The learned Lyapunov NN is used as the terminal cost for the MPC to obtain closed-loop stability and a robustness margin to model errors. To the best of our knowledge, this is the first time such a framework is presented. Using our approach, we show that the size of the stable region increases compared to a baseline MPC that has a longer prediction horizon. By treating the learned Lyapunov NN as a value function estimate, we provide theoretical results for the performance of an MPC with an imperfect forward model. These results complement the ones by Lowrey et al. (2018), which only consider the case when a perfect dynamics model is available.

**Summary of experiments** We demonstrate our approach on constrained non-linear continuous control tasks: a torque-limited inverted pendulum and a non-holonomic vehicle kinematics. We show that our approach can successfully transfer between an inaccurate surrogate and a nominal model, outperforming a long horizon MPC demonstrator.

---

<sup>\*</sup>Equal contribution <sup>1</sup>NNAISENSE, Lugano, Switzerland <sup>2</sup>ETH, Zurich, Switzerland. Correspondence to: Mayank Mittal <mittalma@ethz.ch>, Marco Gallieri <marco@nnaisense.com>.

## 2. Preliminaries

**Controlled Dynamical System** Let us consider a discrete-time, time-invariant, deterministic dynamical system of the form:

$$x(t+1) = f(x(t), u(t)), \quad y(t) = x(t), \quad (1)$$

where  $t \in \mathbb{N}$  is the timestep index,  $x(t) \in \mathbb{R}^{n_x}$ ,  $u(t) \in \mathbb{R}^{n_u}$  and  $y(t) \in \mathbb{R}^{n_y}$  are, respectively, the state, control input, and measurement at timestep  $t$ . We assume that the states and measurements are equivalent. Further, the system described by Equation (1) is subjected to closed and bounded, convex constraints over the state and input spaces. These specifications can be compactly denoted as:

$$x(t) \in \mathbb{X} \subseteq \mathbb{R}^{n_x}, \quad u(t) \in \mathbb{U} \subseteq \mathbb{R}^{n_u}, \quad \forall t > 0. \quad (2)$$

The system is to be controlled by a feedback policy,  $K : \mathbb{R}^{n_x} \rightarrow \mathbb{R}^{n_u}$ , its closed-loop behaviour being defined by  $x(t+1) = f(x(t), K(x(t))) = f_K(x(t))$ . The policy  $K$  is considered *safe* if there exists an invariant set,  $\mathbb{X}_s \subseteq \mathbb{X}$ , for the closed-loop dynamics, inside the constraints. The set  $\mathbb{X}_s$  is also referred to as the *safe-set* for  $f_K$ . Namely, every trajectory for the system  $f_K$  that starts at some  $x \in \mathbb{X}_s$  remains inside this set. Furthermore, if  $x$  asymptotically reaches the equilibrium/target state,  $\bar{x} \in \mathbb{X}_s$ , then  $\mathbb{X}_s$  is also a Region of Attraction (ROA).

**Lyapunov Functions** Lyapunov functions are positive scalar functions of the state,  $V : \mathbb{R}^{n_x} \rightarrow \mathbb{R}^+$ , which monotonically decrease along the closed-loop trajectory of a controlled system until a target point (or set) is reached. The existence of such a function is a necessary and sufficient condition for stability and convergence of dynamical systems (Khalil, 2014). Candidate Lyapunov Functions (or Control Lyapunov Functions) can be used to design control policies, for instance, through direct numerical optimization (Blanchini & Miani, 2007), for piece-wise linear dynamics. The quest for a general solution to non-linear Lyapunov-based constrained control design is still open.

**Lyapunov Conditions** In order to leverage the representational power of neural networks to approximate a Lyapunov function, the learned function must satisfy two conditions. The first requirement for the candidate function is to be upper and lower bounded by strictly increasing, unbounded, positive ( $\mathcal{K}_\infty$ ) functions (Khalil, 2014). In the context of optimal control with a stage cost:

$$\ell(x, u) = x^T Q x + u^T R u, \quad Q \succeq 0, \quad R \succ 0, \quad (3)$$

a possible choice for a  $\mathcal{K}_\infty$ -function is the scaled sum-of-squares of the states:

$$l_\ell \|x\|_2^2 \leq V(x) \leq L_V \|x\|_2^2, \quad (4)$$

<sup>1</sup>In general,  $V(x - \bar{x})$ , where  $\bar{x}$  is a target state. For notation convenience, we set  $\bar{x} = 0$ .

where  $l_\ell$  and  $L_V$  are the minimum eigenvalue of  $Q$  and a (possibly local) Lipschitz constant for  $V$  respectively.

The second and a more important condition is that  $V(x)$  must decrease along the closed-loop system  $f_K(x)$ . A common condition that relates to the Bellman equation in optimal control is that,  $\forall x(t) \in \mathbb{X}_s$  and  $u(t) = K(x(t))$ , the following should be true:

$$V(x(t+1)) - V(x(t)) \leq -\ell(x(t), u(t)). \quad (5)$$

Here  $\mathbb{X}_s$  is the the safe-set as described earlier. For a valid Lyapunov function  $V$ , the safe-set can be defined as a level-set of  $V$ :

$$\mathbb{X}_s = \{x \in \mathbb{X} : V(x) \leq l_s\}. \quad (6)$$

It is worth noting that, if  $K$  solves an infinite-horizon optimal control problem with the stage cost (3) and  $V$  as its *value function*, then Equation (5) holds with equality and the value function  $V$  is *also* a Lyapunov function.

## 3. Neural Lyapunov MPC

In recent work, Gallieri et al. (2019) proposed an alternating descent method for training a Lyapunov NN along with a control policy. They designed the control policy as a multi-layer perceptron (MLP) with tanh activation functions and initialized the network with a known stabilizing policy  $K_0$ . This design choice is a bottleneck of their approach since having an explicit  $K_0$  is often not possible. To overcome this limitation, we present a novel approach where the control policy  $K(x)$  is a non-linear Model Predictive Controller (MPC) (Maciejowski, 2000; Rawlings & Mayne, 2009; Kouvaritakis & Cannon, 2015; Raković & Levine, 2019). Our method uses an expert policy,  $K_0$ , to only generate an initial dataset of single-step demonstrations. This dataset is then used to learn a stabilizing controller.

In the context of MPC, a function  $V(x)$ , which satisfies the Lyapunov property (5) for some local controller  $K_0$ , is instrumental to formally guarantee stability (Mayne et al., 2000; Limon et al., 2003). We use this insight and build a general Lyapunov function terminal cost for our MPC, based on neural networks. We discuss the formulation of the Lyapunov network and the MPC in Section 3.1 and Section 3.2 respectively. In order to extend the controller's ROA while maintaining a short prediction horizon, an alternate optimization scheme is proposed to tune the parameters of the MPC and re-train the Lyapunov NN. We describe this procedure in Section 3.3 and provide a pseudocode of our approach in Algorithm 1.

### 3.1. Lyapunov Network Learning

We use the Lyapunov function network introduced by Gallieri et al. (2019):

$$V(x) = x^T (l_\ell I + V_{net}(x)^T V_{net}(x)) x, \quad (7)$$

where  $V_{net}(x)$  is a (Lipschitz) feedforward network that produces a  $n_V \times n_x$  matrix. The scalars  $n_V$  and  $l_\ell > 0$  are hyper-parameters. It is easy to verify that Equation (7) satisfies the condition mentioned in Equation (4). In our algorithm, we learn the parameters of the network,  $V_{net}(x)$ , and a safe level,  $l_s$ .

In order to reduce the dependency on the stage cost parameters, instead of enforcing Equation (5), a  $V$  is learned such that:

$$\begin{aligned} \forall x(t) \in \mathbb{X}_s, \quad u(t) &= K(x(t)) \\ \Rightarrow V(x(t+1)) - \lambda V(x(t)) &\leq 0, \end{aligned} \quad (8)$$

where  $\lambda \in [0, 1]$  is a constant. If Equation (8) holds, then the set  $\mathbb{X}_s$  is *positively-invariant* (Blanchini & Miani, 2007; Kerrigan, 2000). Since  $\lambda < 1$ , it is also  $\lambda$ -contractive and the state converges to the origin. Equation (8) allows to learn  $V$  from demonstrations without knowing an explicit parameterization of the demonstrator.

**Loss function** Suppose  $\mathcal{D}_K$  denotes a set of state-action-transition tuples of the form  $(x, u, x^+)$ , where  $x^+$  is the next state obtained from applying the policy  $u = K(x)$ . The Lyapunov network is trained using the following loss:

$$\min_{V_{net}, l_s} \mathbf{E}_{(x, u, x^+) \in \mathcal{D}_K} [J(x, u, x^+)], \quad (9)$$

where:

$$J(x, u, x^+) = \frac{\mathcal{I}_{\mathbb{X}_s}(x)}{\rho} J_s(x, u, x^+) + J_{vol}(x, u, x^+), \quad (10)$$

and:

$$\begin{aligned} \mathcal{I}_{\mathbb{X}_s}(x) &= 0.5 (\text{sign}[l_s - V(x)] + 1), \\ J_s(x, u, x^+) &= \frac{\text{ReLU}[\Delta V(x)]}{V(x) + \epsilon_V}, \\ J_{vol}(x, u, x^+) &= \text{sign}[\Delta V(x)] [l_s - V(x)], \\ \Delta V(x) &= V(x^+) - \lambda V(x) + v \ell(x, u). \end{aligned}$$

In Equation (10),  $\mathcal{I}_{\mathbb{X}_s}$  is the indicator function for the safe set  $\mathbb{X}_s$ , which is multiplied to  $J_s$ , a function that penalises the instability. The term  $J_{vol}$  is a classification loss that tries to compute the correct boundary between the stable and unstable points. It is also instrumental in increasing the safe set volume. The scalars  $\epsilon_V > 0$ ,  $\lambda \in [0, 1]$ ,  $v \in [0, 1]$  and  $\rho > 0$ , are hyper-parameters, where the latter trades off volume for stability. When  $\ell$  is unknown for  $K$ , then we set  $v = 0$ . An additional term could be added to the cost to encourage  $\mathbb{X}_s \subseteq \mathbb{X}$ . We instead choose to scale-down the computed level  $l_s$  a-posteriori, for practical reasons.

The loss (10) extends the one proposed by Berkenkamp et al. (2017) in the sense that only one-step transitions are required, and safe trajectories are not explicitly labeled before training. This loss is also used to tune the MPC parameters.

**Local Lyapunov functions and safety** It is often possible that the trained function  $V$  does not satisfy the Lyapunov condition everywhere. This is not uncommon in control problems that deal with non-linearities and uncertainties or when function approximators are used for generating the control signals. Training a Lyapunov NN with a gradient-based method does not guarantee that Equation (8) is satisfied. In general, it may hold only between two level-sets  $\mathbb{X}_s$ , and  $\mathbb{X}_T = \psi \mathbb{X}_s$ , with  $\psi < 1$ , of  $V$ :

$$\begin{aligned} \forall x(t) \in \mathbb{X}_s \setminus \mathbb{X}_T, \quad u(t) &= K(x(t)) \\ \Rightarrow V(x(t+1)) - \lambda V(x(t)) &\leq 0, \end{aligned} \quad (11)$$

However, if  $V$  does not increase beyond  $l_s$  in  $\psi \mathbb{X}_s$ :

$$\begin{aligned} \forall x(t) \in \mathbb{X}_T, \quad u(t) &= K(x(t)) \\ \Rightarrow V(x(t+1)) &< l_s, \end{aligned} \quad (12)$$

then trajectories starting from  $\mathbb{X}_s$  would remain in  $\mathbb{X}_s$  under the policy used to generate the training data for  $V$ . If instead,  $\mathbb{X}_T$  is invariant, then all the trajectories from the demonstrator would terminate in  $\mathbb{X}_T$ .

Formal verification methods can also be used to check that the Lyapunov conditions are satisfied. We refer the reader to (Gallieri et al., 2019; Bobiti, 2017; Bobiti & Lazar, 2016; Berkenkamp et al., 2017) for a set of verification algorithms.

### 3.2. Neural Lyapunov MPC

It is desirable to learn powerful control policies that can perform setpoint-reaching tasks safely, namely, while respecting constraints on the system state and inputs. At the same time, the policies need to be general and directly aware of the constraints. This motivates the use of Model Predictive Control (MPC) policies. The Lyapunov function network techniques from the previous section can be leveraged to formally enforce stability. The key idea is that one can accept a policy to be only locally optimal, or even sub-optimal, as soon as this would result in safe behavior.

Control solutions based on MPC are particularly powerful due to their potential to exploit the inductive bias arising from the direct use of a surrogate model and well studied constrained optimization methods, e.g., sequential quadratic programming (SQP, Nocedal & Wright (2006)), which makes use of convex optimization steps (Boyd & Vandenberghe, 2004). MPC is a global control policy that solves a local optimal control problem of the form:

$$\begin{aligned} J_{\text{MPC}}^*(x(t)) &= \min_{\underline{u}} \gamma^N \alpha V(\hat{x}(N)) + \sum_{i=0}^{N-1} \gamma^i \ell(\hat{x}(i), \hat{u}(i)) \\ \text{s.t.} \quad \hat{x}(i+1) &= \hat{f}(\hat{x}(i), \hat{u}(i)), \\ \hat{x}(i) &\in \mathbb{X}, \forall i \in [0, N], \\ \hat{u}(i) &\in \mathbb{U}, \forall i \in [0, N-1], \\ \hat{x}(0) &= x(t), \end{aligned} \quad (13)$$

where  $\hat{x}(i)$  and  $\hat{u}(i)$  are the predicted state and the input at  $i$ -steps in the future,  $\mathbf{u} = \{u(i)\}_{i=0}^{N-1}$ , the stage cost  $\ell$  is given by (10),  $\gamma \in (0, 1]$  is a discount factor, the function  $\hat{f}$  is a forward model, the function  $V$  is the terminal cost, in our case a Lyapunov NN from Equation (7), scaled by a factor  $\alpha \geq 1$  to provide stability, and  $x(t)$  is the measured system state at the current time. For practical reasons, state constraints are softened and penalty functions are used, as in (Kerrigan & Maciejowski, 2000). The problem (13) is extended with a set of slack variables,  $\hat{s}(i)$ , for state constraint violation and an additional penalty:

$$\ell_{\mathbb{X}}(s) = \eta_1 s^T s + \eta_2 \|s\|_1, \quad (14)$$

where  $\eta_1 > 0$ ,  $\eta_2 \gg 0$ .

For the MPC, problem (13) is solved online (in real-time) given the current state  $x(t)$ ; then, the first element of the optimal control sequence,  $u^*(0)$ , provides the action for the physical system. Then, a new state is measured, and Equation (13) is again solved, in a *receding horizon*.

**NN-based dynamics model** Neural network models are of particular interest in order to leverage existing pipelines for automatic differentiation, computer vision, and the flexibility offered by the NN formalism. It is quite straightforward to include structural priors in the model (Quaglino et al., 2020; Yıldız et al., 2019; Pozzoli et al., 2019) and to exploit time dependencies (Hochreiter & Schmidhuber, 1997; Gers et al., 2000). Recurrent structures can be very beneficial in reducing the modeling errors over a time horizon, which is key for the MPC success. On the other hand, one-step models can perform quite poorly when unrolled. In practice, prediction horizons can be very long, and it might not be possible to gather sufficient data from demonstrations. Even if this is not the case, every model is imperfect, and errors can accumulate through the prediction window. We analyze the framework performance for a bounded one-step-ahead prediction error,  $w(t)$ , where:

$$w = f(x, u) - \hat{f}(x, u), \quad \|w\|_2 \leq \mu, \quad \forall (x, u) \in \tilde{\mathbb{X}} \times \mathbb{U}, \quad (15)$$

for some compact set of states,  $\tilde{\mathbb{X}} \supseteq \mathbb{X}$ . We assume that both  $f$  and  $\hat{f}$  are Lipschitz in this set with constants  $L_{fx}$ ,  $L_{fu}$ , and  $L_{\hat{f}x}$ ,  $L_{\hat{f}u}$  respectively.

**Stability and safety** Stability of MPC without terminal constraint (undiscounted) has been considered by several authors in the past. The proposed framework is based on the results from the work by Limon et al. (2003), where it was first shown that an appropriate  $\alpha$  can be computed so that the resulting MPC is stable without a constraint on the terminal cost. The stability of discounted infinite-horizon discrete-time optimal control problems was analyzed, for instance,

by Postoyan et al. (2014); Gaitsgory et al. (2015), where it was shown that for  $\gamma$  sufficiently close to 1, the stability of an undiscounted problem could be retained locally.

The intrinsic robustness to bounded additive uncertainty of an MPC (undiscounted) with a nominal forward model and without an explicit representation of uncertainty can be formulated within the framework of Input-to-State Stability (ISS) (Limon et al., 2009). We extend this result to the discounted case. In order to prove this, we make use of the uniform continuity of the model, the MPC and the terminal cost,  $V$ , as done by Limon et al. (2009). Consider the set:

$$\Upsilon_{N,\gamma,\alpha} = \left\{ x \in \mathbb{R}^{n_x} : J_{\text{MPC}}^*(x) \leq \frac{1-\gamma^N}{1-\gamma} d + \gamma^N \alpha l_s \right\} \quad (16)$$

where:

$$d = \inf_{x \notin \mathbb{X}_s} \ell(x, 0). \quad (17)$$

The following result is obtained for a deterministic system (1) in closed loop with the MPC defined by problem (13):

**Lemma 1. Stability and robustness** *Assume that  $V(x)$  satisfies (8), for a given  $\lambda \in [0, 1]$ . Then, for any horizon length  $N \geq 1$  there exist a constant  $\bar{\alpha} \geq 0$ , a minimum discount factor  $\bar{\gamma} \in (0, 1]$ , and a model error bound  $\bar{\mu}$  such that, if  $\alpha \geq \bar{\alpha}$ ,  $\mu \leq \bar{\mu}$  and  $\gamma \geq \bar{\gamma}$ , then,  $\forall x(0) \in \mathcal{R}(\mathbb{X}_s)$ :*

1. *If  $N = 1$ ,  $\mu = 0$ , then the system is asymptotically stable for any  $\gamma > 0$ ,  $\forall x(0) \in \Upsilon_{N,\gamma,\alpha}$ .*
2. *If  $N > 1$ ,  $\mu = 0$ , then the system reaches a set  $\mathbb{B}_\gamma$  that is included in  $\mathbb{X}_s$ . This set increases monotonically with decreasing discount factors,  $\gamma$ ,  $\forall x(0) \in \Upsilon_{N,\gamma,\alpha}$ .*
3. *If  $N > 1$ ,  $\mu = 0$ , and once in  $\mathbb{X}_s$  we switch to the expert policy, then the system is asymptotically stable,  $\forall x(0) \in \Upsilon_{N,\gamma,\alpha}$ .*
4. *If  $\alpha V(x)$  is the global value function for the discounted problem,  $\mu = 0$ , and if  $\mathcal{R}(\mathbb{X}_s) = \mathbb{X}_s$ , then the system is asymptotically stable,  $\forall x(0) \in \Upsilon_{N,\gamma,\alpha}$ .*
5. *If  $\alpha V(x)$  is only the value function in  $\mathbb{X}_s$  for the problem,  $\mu = 0$ , and if  $\mathcal{R}(\mathbb{X}_s) \neq \mathbb{X}_s$ , then the system is asymptotically stable,  $\forall x(0) \in \Upsilon_{N,\gamma,\alpha}$ .*
6. *The MPC has a stability margin. If the MPC uses a surrogate model satisfying Equation (15), then the system is Input-to-State (practically) Stable (ISpS) and there exists a set  $\mathbb{B}_{N,\gamma,\mu}$  such that  $x(t) \rightarrow \mathbb{B}_{N,\gamma,\mu}$ ,  $\forall x(0) \in \beta \Upsilon_{N,\gamma,\alpha}$ , with  $\beta \leq 1$ . This final error bound increases monotonically with the model error,  $\mu$ , and the horizon length,  $N$ , as well as for decreasing discount factors,  $\gamma$ .*

Lemma 1 states that for a given horizon length  $N$  and contraction factor  $\lambda$ , one can find a minimum scaling of the

Lyapunov function  $V$  and a lower bound on the discount factor such that the system under the MPC is stable. Hence, if the model is perfect, then the state would converge to the origin as time progresses. However, if the model is not perfect, then the safety of the system depends on the size of the model error. If this error is less than the maximum tolerable error,  $\mu \leq \bar{\mu}$ , then the system is *safe*. The state would converge to a bound, the size of which increases with the size of the model error, the prediction horizon  $N$ , and is inversely proportional to the scaling  $\alpha$ . In other words, the longer the predictions with an incorrect model, the worse the outcome. Note that the ROA also improves with larger  $\alpha$  and  $\gamma$ . The proof of the lemma is provided in Appendix A.

**MPC solvers and intrinsic robustness** The use of iterative convex optimisation, e.g., iterative LQR (iLQR) Tassa et al. (2012) or Sequential Quadratic Program (SQP) Nocedal & Wright (2006), is convenient for several reasons. A clear advantage of this approach is that, if the model  $\hat{f}$  is Lipschitz and the sub-optimal MPC solution is produced by a sequence of strongly convex optimizations such as in SQP, then the resulting control law  $K(x)$  is also Lipschitz (Bemporad et al., 2000; Darup et al., 2017). This is instrumental for proving the existence of a robust stability margin, namely, to account for the model and solver uncertainties, as shown in Lemma 1. In the same way, when using SQP as a solver, the resulting MPC optimal cost,  $J_{\text{MPC}}^*(x)$  is also Lipschitz. Moreover, it can be bounded by  $\mathcal{K}_\infty$ -functions, in the same form as Equation (4) with appropriate constants. This allows using the MPC optimal cost as a candidate robust Lyapunov function. In general, if the solution is feasible and it can be demonstrated that the optimal cost is uniformly continuous, then the MPC has intrinsic robustness independently of the solver (Limon et al., 2003). We formulate our MPC as an SQP. The implementation details of the same are provided in Appendix B.

**Suboptimal solutions** The use of sub-optimal solvers can be interpreted as an additional disturbance,  $w_{\text{solver}}$ , in the MPC predictions. If an SQP is used, then  $K(x)$  is Lipschitz, and the set of initial states is bounded. Hence the effect of sub-optimality is also going to be bounded and can be treated as in point 6 of Lemma 1.

**Local Lyapunov functions** If the function  $V$  is a Lyapunov function only outside the set  $\mathbb{X}_T$ , then in the worst case, the MPC optimal cost would decrease only when the optimal prediction at time  $N$  is outside  $\mathbb{X}_T$ . This can be used to check for convergence to a set as in point 2 of Lemma 1.

**Performance with surrogate models** Our approach to show the performance with a surrogate model is related to the work by Lowrey et al. (2018). We use  $\alpha V(x)$ , instead of an approximation of the value function for the task de-

fined using the stage cost  $\ell(x, u)$ . The focus of Lowrey et al. (2018) was not on stability but instead on optimality and value function learning. If the estimated value function is not enforced to also be a local Lyapunov function, then the constraint satisfaction and safety can only be guaranteed once the value function training has converged and the learning is completed.

Lowrey et al. (2018) formally characterize the MPC performance with an imperfect value function and provide a sub-optimality bound for perfect models. Building upon Lemma 1, we extend the performance bound provided by Lowrey et al. (2018) to the case of imperfect models.

Let  $\mathbf{E}_{\mathcal{D}}[J_{V^*}(K^*)]$  define the expected infinite-horizon performance of the optimal policy  $K^*$ , evaluated by using the correct value function  $V^*$ , for a task specified by the stage cost in Equation (10). Similarly, let  $\mathbf{E}_{x \in \mathcal{D}}[J_{\text{MPC}}^*(x)]$  define the MPC's expected performance with the learned  $V$ , when a surrogate model is used and  $\mathbf{E}_{x \in \mathcal{D}}[J_{\text{MPC}}^*(x; f)]$  when a perfect model is used with the learned  $V$ . We obtain the following lemma:

**Lemma 2. Performance with imperfect models** *Assume that the value function error is bounded for all  $x$ , namely,  $\|V^*(x) - \alpha V(x)\|_2^2 \leq \epsilon$ , and that the model error satisfies (15), for some  $\mu > 0$ . Then, for any  $\delta > 0$ :*

$$\begin{aligned} & \mathbf{E}_{x \in \mathcal{D}}[J_{\text{MPC}}^*(x)] - \mathbf{E}_{x \in \mathcal{D}}[J_{V^*}^*(x)] \\ & \leq \frac{2\gamma^N \epsilon}{1 - \gamma^N} + \left(1 + \frac{1}{\delta}\right) \|Q\|_2 \sum_{i=0}^{N-1} \gamma^i \left(\sum_{j=0}^{i-1} \bar{L}_f^j\right)^2 \mu^2 \\ & \quad + \left(1 + \frac{1}{\delta}\right) \gamma^N \alpha L_V \left(\sum_{i=0}^{N-1} \bar{L}_f^i\right)^2 \mu^2 + \bar{\psi}(\mu) \\ & \quad + \delta \mathbf{E}_{x \in \mathcal{D}}[J_{\text{MPC}}^*(x; f)], \end{aligned}$$

where  $\bar{L}_f = \min(L_{\hat{f}_x}, L_{f_x})$  and  $\bar{\psi}$  is a  $\mathcal{K}_\infty$ -function representing the constraint penalty terms.

Lemma 2 is related to the result by Asadi et al. (2018) for value-based RL. However, here we do not constrain the Lipschitz constant of the model or the system, which can be open-loop unstable. Moreover, in Lemma 2, we do not assume the MPC optimal cost to be Lipschitz. The proof of the lemma is described in Appendix A.

**MPC auto-tuning** The stability bounds discussed in Lemma 1 can be conservative and their computation is non-trivial. Theoretically, the bigger the  $\alpha$  the larger is the ROA (the safe region) for the MPC, up to its maximum extent. Practically, for a very high  $\alpha$ , the MPC solver may not converge due to ill-conditioning. Good stability and performance can be often achieved by manually tuning the MPC parameters, although this can be time-consuming. In theory, it is possible to use a gradient-based optimization scheme to

tune the MPC parameters thanks to the recent advances in differentiable convex programming (Amos & Kolter, 2017; Agrawal et al., 2019b;a). East et al. (2020) trained a stable MPC for the linear case by differentiating through the LQR solution. For the non-linear case, Amos et al. (2018) trained an MPC without state constraints by differentiating through an iLQR (Tassa et al., 2014). However, these approaches are limited in their scope as they either do not address stability for non-linear systems (if at all addressed), do not explicitly handle state constraints, and require optimality in order to compute the gradients correctly. Initially, by using the tool from Agrawal et al. (2019a) within an SQP scheme, we tried to tune the parameters through gradient-based optimization of the loss (9). These attempts were not successful, as expected from the considerations in Amos et al. (2018). Therefore, for practical reasons, in this work, we perform a grid search over the MPC parameter  $\alpha$ .

### 3.3. Learning algorithm

Our alternate optimization of the Lyapunov NN,  $V(x)$ , and the controller is similar to the one of Gallieri et al. (2019). However, instead of training a NN policy, we tune the scaling  $\alpha$  for  $V(x)$ , used in the MPC (13). Further, we extend their approach by using a dataset of demonstrations,  $\mathcal{D}_{\text{demo}}$ , instead of an explicitly defined initial policy. These are one-step transition tuples,  $(x(0), u(0), x(1))_m$ ,  $m = 1, \dots, M$ , generated by a (possibly unknown) stabilizing policy,  $K_0$ . Unlike in the approach by Berkenkamp et al. (2017),  $V$  is learned without labels. It is also not needed to back-propagate through the forward model during the first computation for  $V$ , differently from Chang et al. (2019).

---

#### Algorithm 1 Neural Lyapunov MPC learning

---

**In:**  $\mathcal{D}_{\text{demo}}$ ,  $\hat{f}$ ,  $\lambda \in [0, 1]$ ,  $\{l_\ell, \epsilon_{\text{ext}}\} > 0$ ,  $\gamma \in (0, 1]$ ,  $N \geq 1$ ,  $\alpha_{\text{list}}$ ,  $N_{\text{ext}}$ ,  $N_V$ ,  $\epsilon_V$ ,  $V_{\text{init}}$ ,  $\ell(x, u)$  (if known),  $v \in [0, 1]$   
**Out:**  $V_{\text{net}}$ ,  $l_s$ ,  $\alpha^*$

---

```

 $\mathcal{D} \leftarrow \mathcal{D}_{\text{demo}}$ 
 $V_{\text{net}} \leftarrow V_{\text{init}}$ 
for  $j = 0 \dots N_V$  do
     $(V_{\text{net}}, l_s) \leftarrow$  Adam step on Equation (9)
for  $i = 0 \dots N_{\text{ext}}$  do
     $l_s \leftarrow (1 + \epsilon_{\text{ext}}) l_s$ 
    for  $\alpha \in \alpha_{\text{list}}$  do
         $U_1^* \leftarrow \text{MPC}(V_{\text{net}}, \hat{f}, \mathcal{D}_{\text{demo}}; \alpha)$ , from Equation (13)
         $\mathcal{D}_{\text{MPC}}(\alpha) \leftarrow \text{one\_step\_sim}(\hat{f}, \mathcal{D}_{\text{demo}}, U_1^*)$ 
         $\mathcal{L}(\alpha) \leftarrow$  Evaluate Equation (9) on  $\mathcal{D}_{\text{MPC}}(\alpha)$ 
     $\alpha^* \leftarrow \arg \min(\mathcal{L}(\alpha))$ 
     $\mathcal{D} \leftarrow \mathcal{D}_{\text{MPC}}(\alpha^*)$ 
     $V_{\text{net}} \leftarrow V_{\text{init}}$  (optional)
    for  $j = 0 \dots N_V$  do
         $(V_{\text{net}}, l_s) \leftarrow$  Adam step on Equation (9)
    
```

---

Once an initial  $V$  is learned from the demonstrations, given a forward model, we tune the MPC parameter  $\alpha$  to minimize the loss defined in Equation (7). This procedure over multiple iterations where after each iteration, the tuned MPC serves as a demonstrator for training the next  $V$  that verifies the MPC in closed-loop with the model. The resulting procedure is outlined in Algorithm 1. Additionally, we select the Lyapunov function and the MPC using the criteria that the percentage of stable points ( $\Delta V < 0$ ) increases and that of unstable points decreases while iterating over  $j$  and  $i$ .

In Algorithm 1, MPC denotes the proposed Neural Lyapunov MPC, while `one_step_sim` denotes a one-step propagation of the MPC action into the system surrogate model. To train the parameters of  $V$  and the level-set  $l_s$ , Adam optimizer is used (Kingma & Ba, 2014). A grid search over the MPC parameter  $\alpha$  is performed. A thorough tuning of all MPC parameters is possible, for instance, by using black-box optimisation methods. This is left for future work.

## 4. Numerical experiments

Through our experiments, we show the following: 1) increase in the safe set for the controller by using our proposed alternate learning algorithm, 2) comparison between the proposed Neural Lyapunov MPC against an MPC with a longer horizon in a nominal environment, and, 3) robustness of our one-step MPC compared to a longer horizon MPC with controllers used in conjunction with a surrogate model.

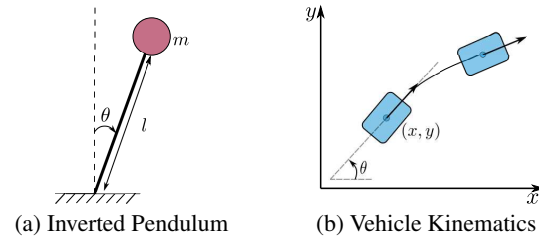


**Figure 1: Non-linear robotic control problems.** We test our approach on: (a) torque-limited inverted pendulum of mass  $m$  and length  $l$ , and (b) non-holonomic vehicle kinematics with constraints.

The proposed approach is verified on two different robotic control problems, shown in Figure 1. In Section 4.1, a torque-limited inverted pendulum is considered while in Section 4.2, we consider a non-holonomic vehicle kinematics with constraints. Details about the models and their configurations can be found in Appendix C.

### 4.1. Inverted pendulum

In this task, the pendulum starts near the unstable equilibrium ( $\theta = 0^\circ$ ). The goal is to stay upright. We bound the input so that the system cannot be stabilized if  $|\theta| > 60^\circ$ .

Table 1: **Inv. Pendulum: Learning on nominal model.**

ITER.	LOSS ( $\log(1+x)$ )	VERIFIED (%)	NOT VERIFIED (%)
1	3.21	13.25	0.00
2	1.08	13.54	0.00

**Setup** We use an MPC with horizon 4 as a demonstrator, with terminal cost,  $500x^T P_{\text{LQR}}x$ , where  $P_{\text{LQR}}$  is the LQR optimal cost matrix. This is evaluated on  $10K$  equally spaced initial states to generate the dataset  $\mathcal{D}_{\text{demo}}$ . We train a grey-box NN model. More details are in Appendix C.

**Results** The learned  $V$  and  $\alpha$ , obtained from Algorithm 1, produce a one-step MPC that stabilizes both the surrogate and the actual system. Table 1 shows that the loss and percentage of verified points improve across iterations. The final ROA estimate is nearly maximal and is depicted along with the safe trajectories, produced by the MPC while using predictions from the nominal and surrogate models, in Figure 2. The performance matches that of the baseline and the transfer is successful due to the accuracy of the learned model. A full ablation study is in Appendix D.

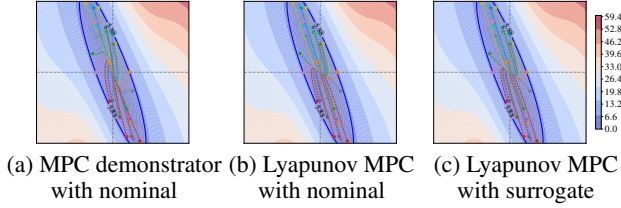


Figure 2: **Inverted Pendulum: Testing learned controller on nominal model.** Lyapunov function with safe trajectories for 80 steps. The learning and transfer are successful.

#### 4.2. Car kinematics

The goal is to steer the car to the  $(0, 0)$  position with zero orientation. This is only possible through non-linear control.

**Setup** The vehicle cannot move sideways, hence policies such as LQR is not usable to generate demonstrations. Thus to create  $\mathcal{D}_{\text{demo}}$ , an MPC with horizon 5 is evaluated over  $10K$  random initial states. The surrogate is a grey-box NN. More details are in Appendix C.

**Results** Figure 3 shows the learning curve for the loss, and the percentages of stable and unstable points, over three iterations using the nominal model for training. All the metrics improve across the iterations, indicating an increase in the ROA. This is summarized in Table 2. Similar results are obtained when learning on the surrogate model, as shown in Table 3. We test the transfer capability of the approach in

two ways. First, we learn using the nominal model and test using the surrogate model for the MPC predictions. This is reported in Figure 4, where it can be noticed that our MPC significantly outperforms the demonstrator when the inaccurate model is used for predictions. Second, the learning is performed using the surrogate model as in Algorithm 1, and the MPC is then tested on the nominal model while still using the surrogate for prediction. This is depicted in Figure 5. Once again, our MPC works better than the demonstrator when using the incorrect model. The learned MPC transfers successfully and completes the task safely.

 Table 2: **Car Kinematics: Learning on nominal model.**

ITER.	LOSS ( $\log(1+x)$ )	VERIFIED (%)	NOT VERIFIED (%)
1	1.55	92.20	4.42
2	0.87	93.17	4.89
3	0.48	94.87	3.89

 Table 3: **Car Kinematics: Learning on surrogate model.**

ITER.	LOSS ( $\log(1+x)$ )	VERIFIED (%)	NOT VERIFIED (%)
1	1.84	91.74	8.26
2	1.43	92.26	7.74
3	1.65	91.61	8.39

## 5. Additional references

In the context of reinforcement learning, Gu et al. (2016) consider the use of local models and quadratic advantage functions to accelerate deep Q-learning. On the other hand, Lowrey et al. (2018) learn a value function and use it with an MPC for a perfect model. They show that this improves both the learning and the performance. We extend their results in Lemma 2 for imperfect models. Farshidian et al. (2019) extend the work by Lowrey et al. (2018) to stochastic MPC in continuous-time. Asadi et al. (2018) provide probabilistic bounds on value error with Lipschitz models, where the Lipschitz constant is limited by the discount factor. Janner et al. (2019) characterize and analyze the performance of policy iteration with imperfect models.

## 6. Conclusion

We presented Neural Lyapunov MPC, a framework to train a stabilizing non-linear MPC based on learned neural network terminal cost and surrogate model. After extending existing theoretical results for MPC and value-based reinforcement learning, we have demonstrated that the proposed framework can incrementally increase the stability region of the MPC and safely transfer on simulated constrained non-linear control scenarios.



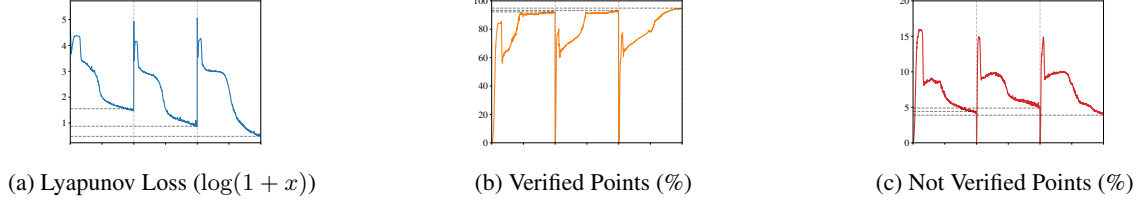


Figure 3: **Car kinematics: Alternate learning on nominal model.** We plot the Lyapunov loss (9) on a  $\log(1 + x)$  scale and indicate its performance as percentage verified and not verified points. Vertical lines separate alternate learning iterations.

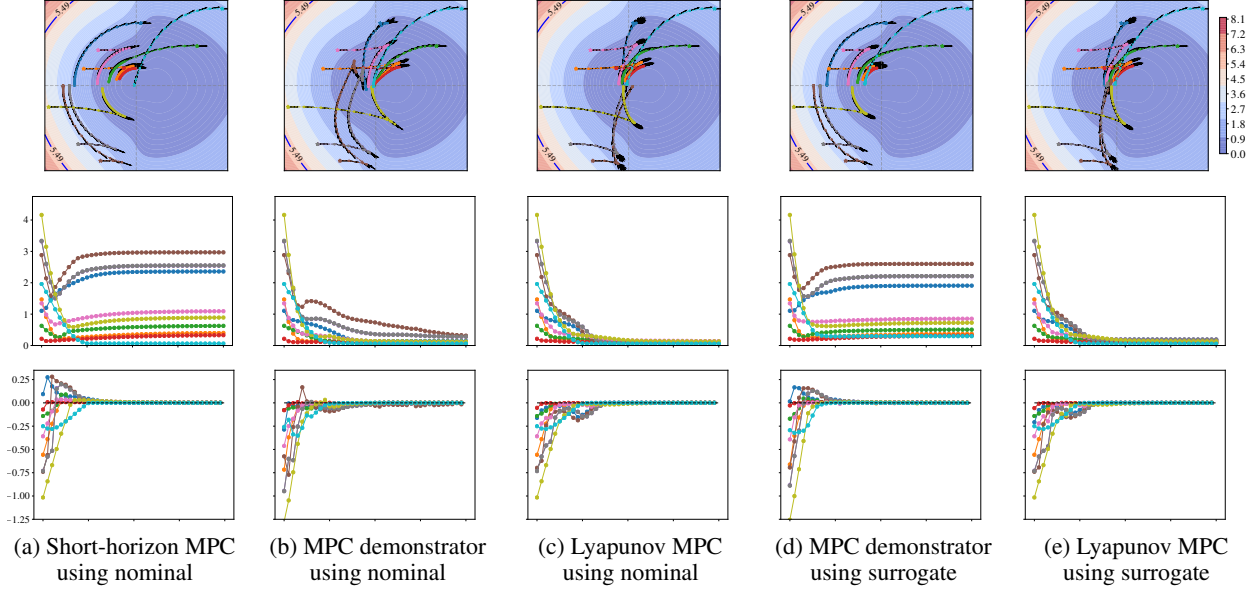


Figure 4: **Car kinematics: Testing learned controller on nominal model.** **Top:** The Lyapunov function at  $\phi = 0$  with trajectories for 40 steps. **Middle:** The evaluated Lyapunov function. **Bottom:** The Lyapunov function time differences.

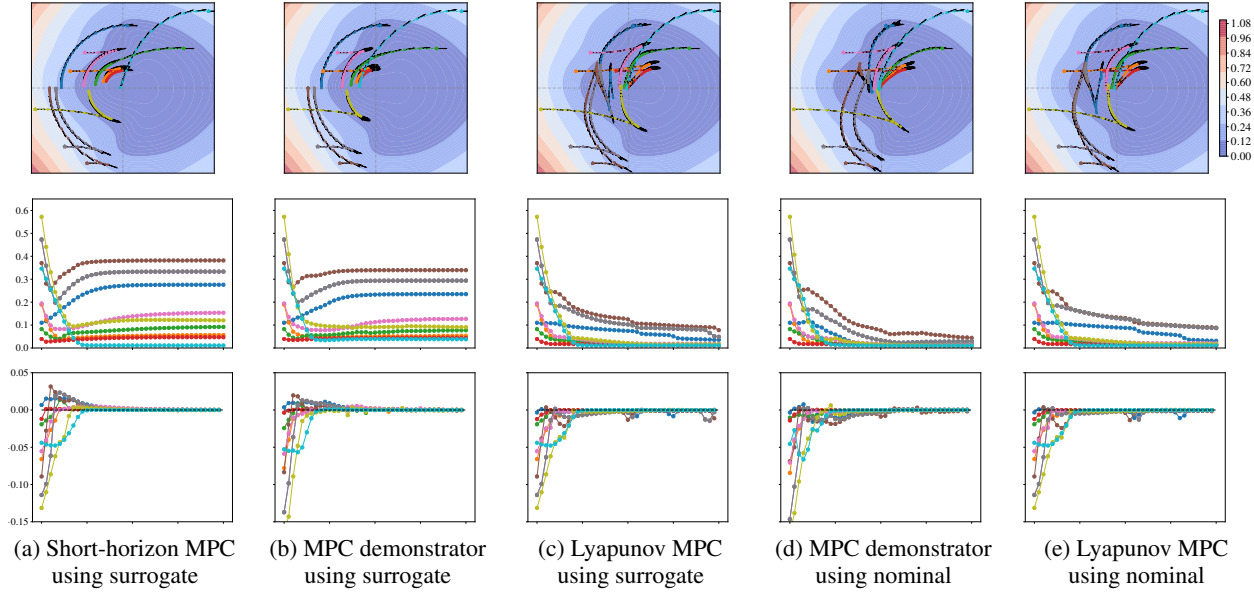


Figure 5: **Car kinematics: Transfer from surrogate to a nominal model.** **Top:** The Lyapunov function at  $\phi = 0$  with trajectories for 40 steps. **Middle:** The evaluated Lyapunov function. **Bottom:** The Lyapunov function time differences.



## References

- Agrawal, A., Amos, B., Barratt, S., Boyd, S., Diamond, S., and Kolter, Z. Differentiable Convex Optimization Layers. *arXiv:1910.12430 [cs, math, stat]*, October 2019a. URL <http://arxiv.org/abs/1910.12430>. arXiv: 1910.12430.
- Agrawal, A., Barratt, S., Boyd, S., Busseti, E., and Moursi, W. M. Differentiating Through a Cone Program. *arXiv:1904.09043 [math]*, April 2019b. URL <http://arxiv.org/abs/1904.09043>. arXiv: 1904.09043.
- Amos, B. and Kolter, J. Z. OptNet: Differentiable Optimization as a Layer in Neural Networks. *arXiv:1703.00443 [cs, math, stat]*, March 2017. URL <http://arxiv.org/abs/1703.00443>. arXiv: 1703.00443.
- Amos, B., Jimenez, I., Sacks, J., Boots, B., and Kolter, J. Z. Differentiable MPC for End-to-end Planning and Control. In *Advances in Neural Information Processing Systems 31*, pp. 8289–8300. Curran Associates, Inc., 2018.
- Asadi, K., Misra, D., and Littman, M. L. Lipschitz Continuity in Model-based Reinforcement Learning. *arXiv:1804.07193 [cs, stat]*, July 2018. URL <http://arxiv.org/abs/1804.07193>. arXiv: 1804.07193.
- Bemporad, A., Morari, M., Dua, V., and Pistikopoulos, E. The explicit solution of model predictive control via multiparametric quadratic programming. In *Proceedings of the American Control Conference*. IEEE, 2000. URL <https://doi.org/10.1109/acc.2000.876624>.
- Berkenkamp, F., Turchetta, M., Schoellig, A. P., and Krause, A. Safe Model-based Reinforcement Learning with Stability Guarantees. *arXiv:1705.08551 [cs, stat]*, May 2017. URL <http://arxiv.org/abs/1705.08551>. arXiv: 1705.08551.
- Blanchini, F. and Miani, S. *Set-Theoretic Methods in Control (Systems & Control: Foundations & Applications)*. Birkhäuser, 2007. ISBN 0817632557.
- Bobiti, R. and Lazar, M. Sampling-based verification of Lyapunov’s inequality for piecewise continuous nonlinear systems. *arXiv:1609.00302 [cs]*, September 2016. URL <http://arxiv.org/abs/1609.00302>. arXiv: 1609.00302.
- Bobiti, R. V. *Sampling driven stability domains computation and predictive control of constrained nonlinear systems*. PhD thesis, 2017. URL [https://pure.tue.nl/ws/files/78458403/20171025\\_Bobiti.pdf](https://pure.tue.nl/ws/files/78458403/20171025_Bobiti.pdf).
- Boyd, S. and Vandenberghe, L. *Convex Optimization*. Cambridge University Press, 2004. ISBN 0521833787.
- Chang, Y.-C., Roohi, N., and Gao, S. Neural Lyapunov Control. In *Advances in Neural Information Processing Systems*, pp. 3240–3249. 2019. URL <http://papers.nips.cc/paper/8587-neural-lyapunov-control.pdf>.
- Darup, M. S., Jost, M., Pannocchia, G., and Mönnigmann, M. On the maximal controller gain in linear MPC. *20th IFAC World Congress*, 50(1):9218–9223, July 2017.
- East, S., Gallieri, M., Masci, J., Koutnik, J., and Cannon, M. Infinite-Horizon Differentiable Model Predictive Control. *arXiv:2001.02244 [cs, eess, math]*, January 2020. URL <http://arxiv.org/abs/2001.02244>. arXiv: 2001.02244.
- Farshidian, F., Hoeller, D., and Hutter, M. Deep Value Model Predictive Control. *arXiv:1910.03358 [cs, stat]*, October 2019. URL <http://arxiv.org/abs/1910.03358>. arXiv: 1910.03358.
- Fossen, T. I. *Handbook of marine craft hydrodynamics and motion control*. John Wiley & Sons, 2011.
- Gaitsgory, V., Gruene, L., and Thatcher, N. Stabilization with discounted optimal control. volume 82, pp. 91–98, 07 2015. doi: 10.1016/j.sysconle.2015.05.010.
- Gallieri, M., Salehian, S. S. M., Toklu, N. E., Quaglino, A., Masci, J., Koutník, J., and Gomez, F. Safe Interactive Model-Based Learning. *arXiv:1911.06556 [cs, eess]*, November 2019. URL <http://arxiv.org/abs/1911.06556>. arXiv: 1911.06556.
- Gers, F. A., Schmidhuber, J., and Cummins, F. Learning to forget: Continual prediction with LSTM. *Neural Computation*, 12(10):2451–2471, 2000.
- Glorot, X. and Bengio, Y. Understanding the difficulty of training deep feedforward neural networks. In Teh, Y. W. and Titterton, M. (eds.), *Proceedings of the International Conference on Artificial Intelligence and Statistics*, volume 9 of *Proceedings of Machine Learning Research*, pp. 249–256, Chia Laguna Resort, Sardinia, Italy, 13–15 May 2010. PMLR.
- Gu, S., Lillicrap, T., Sutskever, I., and Levine, S. Continuous deep q-learning with model-based acceleration. 03 2016.
- Hadfield-Menell, D., Lin, C., Chitnis, R., Russell, S., and Abbeel, P. Sequential quadratic programming for task plan optimization. In *Proceedings of IEEE/RSJ International Conference on Intelligent Robots and Systems*, pp. 5040–5047. IEEE, 2016.

- Hochreiter, S. and Schmidhuber, J. Long short-term memory. *Neural Computation*, 9(8):1735–1780, 1997.
- Janner, M., Fu, J., Zhang, M., and Levine, S. When to Trust Your Model: Model-Based Policy Optimization. *arXiv:1906.08253 [cs, stat]*, November 2019. URL <http://arxiv.org/abs/1906.08253>. arXiv: 1906.08253.
- Kerrigan, E. Robust constraint satisfaction: Invariant sets and predictive control. Technical report, 2000. URL <http://hdl.handle.net/10044/1/4346>.
- Kerrigan, E. C. and Maciejowski, J. M. Soft constraints and exact penalty functions in model predictive control. In *Proceedings of UKACC International Conference*, 2000.
- Khalil, H. K. *Nonlinear Control*. Pearson, 2014. ISBN 9780133499261.
- Kingma, D. P. and Ba, J. Adam: A Method for Stochastic Optimization. *arXiv:1412.6980 [cs]*, December 2014. URL <http://arxiv.org/abs/1412.6980>. arXiv: 1412.6980.
- Kouvaritakis, B. and Cannon, M. *Model Predictive Control: Classical, Robust and Stochastic*. Advanced Textbooks in Control and Signal Processing, Springer, London, 2015.
- Limon, D., Alamo, T., and Camacho, E. F. Stable constrained MPC without terminal constraint. *Proceedings of the American Control Conference*, 2003.
- Limon, D., Alamo, T., Raimondo, D. M., de la Peña, D. M., Bravo, J. M., Ferramosca, A., and Camacho, E. F. Input-to-State Stability: A Unifying Framework for Robust Model Predictive Control. In *Nonlinear Model Predictive Control*, pp. 1–26. Springer Berlin Heidelberg, 2009.
- Lowrey, K., Rajeswaran, A., Kakade, S., Todorov, E., and Mordatch, I. Plan Online, Learn Offline: Efficient Learning and Exploration via Model-Based Control. *arXiv:1811.01848 [cs, stat]*, November 2018. URL <http://arxiv.org/abs/1811.01848>. arXiv: 1811.01848.
- Maciejowski, J. *Predictive Control with Constraints*. Prentice Hall, 2000. ISBN 0201398230.
- Mayne, D., Rawlings, J., Rao, C., and Sokaert, P. Constrained model predictive control: Stability and optimality. *Automatica*, 36(6):789 – 814, 2000.
- Nocedal, J. and Wright, S. *Numerical optimization*. Springer Science & Business Media, 2006.
- Paszke, A., Gross, S., Massa, F., Lerer, A., Bradbury, J., Chanan, G., Killeen, T., Lin, Z., Gimelshein, N., Antiga, L., Desmaison, A., Köpf, A., Yang, E., DeVito, Z., Raison, M., Tejani, A., Chilamkurthy, S., Steiner, B., Fang, L., Bai, J., and Chintala, S. Pytorch: An imperative style, high-performance deep learning library, 2019. URL <http://arxiv.org/abs/1912.01703>.
- Postoyan, R., Busoniu, L., Nesić, D., and Daafouz, J. Stability of infinite-horizon optimal control with discounted cost. In *Proceedings of the IEEE Conference on Decision and Control*, 2014.
- Pozzoli, S., Gallieri, M., and Scattolini, R. Tustin neural networks: a class of recurrent nets for adaptive MPC of mechanical systems. *arXiv:1911.01310 [cs, eess]*, November 2019. URL <http://arxiv.org/abs/1911.01310>. arXiv: 1911.01310.
- Quaglino, A., Gallieri, M., Masci, J., and Koutník, J. SNODE: Spectral Discretization of Neural ODEs for System Identification. *arXiv:1906.07038 [cs]*, January 2020. URL <http://arxiv.org/abs/1906.07038>. arXiv: 1906.07038.
- Raković, S. V. and Levine, W. S. (eds.). *Handbook of Model Predictive Control*. Springer International Publishing, 2019. doi: 10.1007/978-3-319-77489-3. URL <https://doi.org/10.1007/978-3-319-77489-3>.
- Rawlings, J. B. and Mayne, D. Q. *Model Predictive Control Theory and Design*. Nob Hill Pub, Llc, 2009. ISBN 0975937707.
- Tassa, Y., Erez, T., and Todorov, E. Synthesis and stabilization of complex behaviors through online trajectory optimization. In *Proceedings of the IEEE/RSJ International Conference on Intelligent Robots and Systems.*, pp. 4906–4913, 10 2012. ISBN 978-1-4673-1737-5. doi: 10.1109/IROS.2012.6386025.
- Tassa, Y., Mansard, N., and Todorov, E. Control-limited differential dynamic programming. In *Proceedings of IEEE International Conference on Robotics and Automation*, pp. 1168–1175, 2014. doi: 10.1109/ICRA.2014.6907001.
- Yıldız, C., Heinonen, M., and Lähdesmäki, H. ODE<sup>2</sup>VAE: Deep generative second order ODEs with Bayesian neural networks. *arXiv:1905.10994 [cs, stat]*, October 2019. URL <http://arxiv.org/abs/1905.10994>. arXiv: 1905.10994.

---

# Neural Lyapunov Model Predictive Control

## Supplementary Material

---

Mayank Mittal <sup>\*1,2</sup> Marco Gallieri <sup>\*1</sup> Alessio Quaglino <sup>1</sup> Seyed Sina Mirrazavi Salehian <sup>1</sup> Jan Koutník <sup>1</sup>

### A. Proof of the Lemmas

Here we provide the proofs of lemmas stated in the paper. We write the proof for Lemma 2 before Lemma 1 since it is simpler and helps in proving the latter.

#### Proof of Lemma 2

*Proof.* To prove the lemma, we first write:

$$\begin{aligned} \mathbf{E}_{x \in \mathcal{D}}[J_{\text{MPC}}^*(x)] - \mathbf{E}_{x \in \mathcal{D}}[J_{V^*}^*(x)] &= \\ &\underbrace{\mathbf{E}_{x \in \mathcal{D}}[J_{\text{MPC}}^*(x)] - \mathbf{E}_{x \in \mathcal{D}}[J_{\text{MPC},f}^*(x)]}_{I_1} + \\ &\underbrace{\mathbf{E}_{x \in \mathcal{D}}[J_{\text{MPC},f}^*(x)] - \mathbf{E}_{x \in \mathcal{D}}[J_{V^*}^*(x)]}_{I_2}, \end{aligned} \quad (18)$$

where  $\mathbf{E}_{x \in \mathcal{D}}[J_{\text{MPC},f}^*(x)]$  denotes the MPC performance when a perfect model is used for predictions.

For the term  $I_2$ , Lowrey et al. (2018) provide a bound on the performance of the MPC policy. It is important to note that in their problem formulation, the MPC's objective is defined as a maximization over the cumulative discounted reward, while in our formulation (13) we consider a minimization over the cost. Consequently, compared to inequality presented by Lowrey et al. (2018), there is a change in sign of the terms in the left-hand side of the inequality. This means:

$$\mathbf{E}_{x \in \mathcal{D}}[J_{\text{MPC},f}^*(x)] - \mathbf{E}_{x \in \mathcal{D}}[J_{V^*}^*(x)] \leq \frac{2\gamma^N \epsilon}{1 - \gamma^N}. \quad (19)$$

We now focus on the term  $I_1$  in Equation (18). Let us denote  $x^*(i)$  and  $u^*(i)$  as the optimal state and action predictions respectively, obtained by using the correct model,  $f$ , and the MPC policy at time  $i$ . By the principle of optimality, the optimal sequence for the MPC using the correct model,  $\underline{u}_f$ , can be used to upper-bound the optimal cost for the MPC using the surrogate model:

$$\begin{aligned} \mathbf{E}_{x \in \mathcal{D}}[J_{\text{MPC}}^*(x)] - \mathbf{E}_{x \in \mathcal{D}}[J_{\text{MPC},f}^*(x)] &\leq \\ \mathbf{E}_{x \in \mathcal{D}}[J_{\text{MPC}}(x, \underline{u}_f)] - \mathbf{E}_{x \in \mathcal{D}}[J_{\text{MPC},f}^*(x)]. \end{aligned} \quad (20)$$

Since the input sequence is now the same for both terms in right-hand side of Equation (20), the difference in the

cost is driven by the different state trajectories cost (the cost on  $x$  over the horizon which includes the state-constraint violation penalty, as defined in Equation (14)) as well as the terminal cost. In form of equation, this means:

$$\begin{aligned} \mathbf{E}_{x \in \mathcal{D}}[J_{\text{MPC}}(x, \underline{u}_f)] - \mathbf{E}_{x \in \mathcal{D}}[J_{\text{MPC},f}^*(x)] &= \\ &\mathbf{E}_{x \in \mathcal{D}}[J_{\text{MPC}}(x, \underline{u}_f) - J_{\text{MPC},f}^*(x)] \\ &= \mathbf{E}_{x(0) \in \mathcal{D}} \left[ \sum_{j=0}^{N-1} \gamma^j \left\{ \hat{x}(j)^T Q \hat{x}(j) - x^*(j)^T Q x^*(j) \right\} \right. \\ &\quad \left. + \gamma^N \alpha \{ V(\hat{x}(N)) - V(x^*(N)) \} \right. \\ &\quad \left. + \sum_{j=0}^N \{ \ell_{\mathbb{X}}(\hat{x}(j)) - \ell_{\mathbb{X}}(x^*(j)) \} \right]. \end{aligned} \quad (21)$$

Recall that we assume the surrogate model is Lipschitz with constant  $L_{\hat{f}_x}$ . This means that  $\forall \tilde{x}, x \in \mathbb{R}^{n_x}$  and the same input  $u \in \mathbb{R}^{n_u}$ , we have:

$$\|\hat{f}(\tilde{x}, u) - \hat{f}(x, u)\|_2 \leq L_{\hat{f}_x} \|\tilde{x} - x\|_2,$$

Further, from Equation (15),  $\forall (x, u) \in \tilde{\mathbb{X}} \times \mathbb{U}$ , we have:

$$\|w(x, u)\|_2 = \|f(x, u) - \hat{f}(x, u)\|_2 \leq \mu.$$

Under the optimal policy for the correct model, let us denote the deviation in the state prediction when the MPC input prediction is applied with a different model,  $\hat{f}$ , as  $\hat{d}(j) := \hat{x}(j) - x^*(j)$ .

At step  $j = 1$ :

$$\begin{aligned} \|\hat{d}(1)\|_2 &= \|\hat{x}(1) - x^*(1)\|_2 \\ &= \|\hat{f}(x^*(0), u^*(0)) - f(x^*(0), u^*(0))\|_2 \\ &= \|w(x^*(0), u^*(0))\|_2 \\ &\leq \mu. \end{aligned}$$

At step  $j = 2$ :

$$\begin{aligned}
 \|\hat{d}(2)\|_2 &= \|\hat{x}(2) - x^*(2)\| \\
 &= \|\hat{f}(x^*(1) + \hat{d}(1), u^*(1)) - f(x^*(1), u^*(1))\| \\
 &= \|\hat{f}(x^*(1) + \hat{d}(1), u^*(1)) - \hat{f}(x^*(1), u^*(1)) \\
 &\quad + \hat{f}(x^*(1), u^*(1)) - f(x^*(1), u^*(1))\| \\
 &\leq \underbrace{\|\hat{f}(x^*(1) + \hat{d}(1), u^*(1)) - \hat{f}(x^*(1), u^*(1))\|}_{\leq L_{\hat{f}x} \|\hat{d}(1)\|} \\
 &\quad + \underbrace{\|\hat{f}(x^*(1), u^*(1)) - f(x^*(1), u^*(1))\|}_{= \|w(x^*(1), u^*(1))\| \leq \mu} \\
 &\leq L_{\hat{f}x} \mu + \mu
 \end{aligned}$$

By induction, it can be shown that:

$$\|\hat{d}(j)\|_2 = \|\hat{x}(j) - x^*(j)\| \leq \sum_{i=0}^{j-1} L_{\hat{f}x}^i \mu. \quad (22)$$

Alternately, if we assume the correct system that is to be controlled is Lipschitz with constant  $L_{fx}$ , then proceeding as before:

At step  $j = 1$ :

$$\begin{aligned}
 \|\hat{d}(1)\|_2 &= \|\hat{x}(1) - x^*(1)\|_2 \\
 &\leq \mu.
 \end{aligned}$$

At step  $j = 2$ :

$$\begin{aligned}
 \|\hat{d}(2)\|_2 &= \|\hat{x}(2) - x^*(2)\| \\
 &= \|\hat{f}(\hat{x}(1), u^*(1)) - f(\hat{x}(1) - \hat{d}(1), u^*(1))\| \\
 &\leq \underbrace{\|\hat{f}(\hat{x}(1), u^*(1)) - f(\hat{x}(1), u^*(1))\|}_{= \|w(\hat{x}(1), u^*(1))\| \leq \mu} \\
 &\quad + \underbrace{\|\hat{f}(\hat{x}(1), u^*(1)) - f(\hat{x}(1) - \hat{d}(1), u^*(1))\|}_{\leq L_{fx} \|\hat{d}(1)\|} \\
 &\leq \mu + L_{fx} \mu
 \end{aligned}$$

By induction, again we have:

$$\|\hat{d}(j)\|_2 = \|\hat{x}(j) - x^*(j)\| \leq \sum_{i=0}^{j-1} L_{fx}^i \mu. \quad (23)$$

Combining equations (22) and (23) and by letting  $\bar{L}_f^i = \min(L_{\hat{f}x}^i, L_{fx}^i)$ , we obtain:

$$\|\hat{d}(j)\|_2 = \|\hat{x}(j) - x^*(j)\| \leq \sum_{i=0}^{j-1} \bar{L}_f^i \mu. \quad (24)$$

The following identity is used;  $\forall \delta > 0$ :

$$\|a + b\|_2^2 \leq \left(1 + \frac{1}{\delta}\right) \|a\|_2^2 + (1 + \delta) \|b\|_2^2.$$

Hence, we can write the cost over the predicted state as:

$$\begin{aligned}
 &\hat{x}(j)^T Q \hat{x}(j) \\
 &= \|Q^{1/2} \hat{x}(j)\|_2^2 = \|Q^{1/2} (x^*(j) + \hat{d}(j))\|_2^2 \\
 &\leq (1 + \delta) \|Q^{1/2} x^*(j)\|_2^2 + \left(1 + \frac{1}{\delta}\right) \|Q^{1/2} \hat{d}(j)\|_2^2 \\
 &\leq (1 + \delta) x^*(j)^T Q x^*(j) + \left(1 + \frac{1}{\delta}\right) \|Q\|_2 \|\hat{d}(j)\|_2^2.
 \end{aligned} \quad (25)$$

From equations (24) and (25),  $\forall j \in \{0, 1, \dots, N-1\}$ , we obtain:

$$\begin{aligned}
 &\hat{x}(j)^T Q \hat{x}(j) - x^*(j)^T Q x^*(j) \\
 &\leq \underbrace{\delta x^*(j)^T Q x^*(j)}_{= \ell(x^*(j), 0)} + \left(1 + \frac{1}{\delta}\right) \|Q\|_2 \left(\sum_{i=0}^{j-1} \bar{L}_f^i \mu\right)^2 \\
 &\leq \delta \ell(x^*(i), u^*(i)) + \left(1 + \frac{1}{\delta}\right) \|Q\|_2 \left(\sum_{i=0}^{j-1} \bar{L}_f^i \mu\right)^2.
 \end{aligned} \quad (26)$$

Recall from Equation (4) that  $V(x) \leq L_V \|x\|_2^2$ . Proceeding as before, we can write the following for the terminal cost:

$$\begin{aligned}
 &V(\hat{x}(N)) - V(x^*(N)) \\
 &\leq \delta V(x^*(N)) + \left(1 + \frac{1}{\delta}\right) L_V \left(\sum_{i=0}^{N-1} \bar{L}_f^i \mu\right)^2.
 \end{aligned} \quad (27)$$

The final part of the proof concerns the constraints cost term. Let the state constraints be defined as a set of inequalities:

$$\mathbb{X} = \{x \in \mathbb{R}^n : g(x) \leq 1\},$$

where  $g$  is a convex function. For the optimal solution,  $x^*$ , the violation of the constraint is represented through the slack variable:

$$s^* = s(x^*) = \frac{(g(x^*) - 1) + |g(x^*) - 1|}{2}.$$

Since the constraints are convex and compact, and they contain the origin, then at the optimal solution,  $x^*$ , we have that there exists a  $\mathcal{K}_\infty$ -function,  $\bar{\eta}(r)$ , such that:

$$\left| \ell_{\mathbb{X}}(s(x^* + \hat{d})) - \ell_{\mathbb{X}}(s(x^*)) \right| \leq \bar{\eta}(\|\hat{d}\|).$$

Using the above inequality and Equation (24), it follows that,  $\forall j \in \{0, 1, \dots, N\}$ :

$$\ell_{\mathbb{X}}(\hat{x}(j)) - \ell_{\mathbb{X}}(x^*(j)) \leq \bar{\eta} \left( \sum_{i=0}^{j-1} \bar{L}_f^i \mu \right) = \bar{\eta}_j. \quad (28)$$

By combining equations (18), (19), (20), (21), (26), (27) and (28), we obtain the bound stated in the lemma:

$$\begin{aligned} & \mathbf{E}_{x \in \mathcal{D}}[J_{\text{MPC}}^*(x)] - \mathbf{E}_{x \in \mathcal{D}}[J_{V^*}^*(x)] \\ & \leq \frac{2\gamma^N \epsilon}{1 - \gamma^N} + \left(1 + \frac{1}{\delta}\right) \|Q\|_2 \sum_{i=0}^{N-1} \gamma^i \left( \sum_{j=0}^{i-1} \bar{L}_f^j \right)^2 \mu^2 \\ & \quad + \left(1 + \frac{1}{\delta}\right) \gamma^N \alpha L_V \left( \sum_{i=0}^{N-1} \bar{L}_f^i \right)^2 \mu^2 + \underbrace{\sum_{j=0}^N \bar{\eta}_j}_{=: \bar{\psi}(\mu)} \\ & \quad + \delta \mathbf{E}_{x \in \mathcal{D}}[J_{\text{MPC}}^*(x; f)]. \end{aligned}$$

□

### Proof of Lemma 1

*Proof.* In order to prove point 1 in the lemma, we first use the standard arguments for the MPC without terminal constraint (Mayne et al., 2000; Limon et al., 2003) in the undiscounted case. We then extend the results to the discounted case.

**Nominal stability** First, when an invariant set terminal constraint is used, which in our case corresponds to the condition  $V(x(N)) \leq l_s$  with  $\mathbb{X}_s \subseteq \mathbb{X}$ , then Mayne et al. (2000) have provided conditions to prove stability by demonstrating that  $J_{\text{MPC}}^*(x)$  is a Lyapunov function. These require the terminal cost to be a Lyapunov function that satisfies Equation (5). Hence, we start by looking for values of  $\alpha$  such that  $\alpha V(x)$  satisfies Equation (5). In other words, we wish to find an  $\bar{\alpha}_1 \geq 1$  such that, for all  $\alpha \geq \bar{\alpha}_1$  and for some policy  $K_0$  (in our case, the demonstrator for  $V$ ), the following condition holds:

$$\alpha V(f(x, K_0(x))) - \alpha V(x) \leq -\ell(x, K_0(x)). \quad (29)$$

Let us denote  $x^+ = f(x, K_0(x))$  for brevity. We have, by assumption, that:

$$\alpha(V(x^+) - \lambda V(x)) \leq 0. \quad (30)$$

This implies that:

$$\begin{aligned} & \alpha V(x^+) - \alpha V(x) + \alpha V(x) - \alpha \lambda V(x) \leq 0, \\ \Rightarrow & \alpha V(x^+) - \alpha V(x) \leq -\alpha(1 - \lambda)V(x). \end{aligned} \quad (31)$$

Recall that the loss function satisfies  $l_\ell \|x\|_2^2 \leq \ell(x, u)$ . Since the MPC is solved using a sequence of convex quadratic programs, it is also Lipschitz (Bemporad et al., 2000). Similarly, if  $K_0$  is Lipschitz or (uniformly) continuous over the closed and bounded set  $\mathbb{U}$ , then since  $\mathbb{X}$  is also closed and bounded, there also exists a local upper bound for the loss function on this policy, namely,  $\ell(x, K_0(x)) \leq L_\ell \|x\|_2^2$ .

Further, recall from Equation (4) that  $l_\ell \|x\|_2^2 \leq V(x)$ . Using the above notions, we have:

$$\begin{aligned} \alpha V(x^+) - \alpha V(x) & \leq -\alpha(1 - \lambda)l_\ell \|x\|_2^2, \\ & = -\alpha(1 - \lambda)l_\ell \frac{L_\ell}{L_\ell} \|x\|_2^2 \\ & \leq -\frac{\alpha(1 - \lambda)l_\ell}{L_\ell} \ell(x, K_0(x)) \\ & = -\beta \ell(x, K_0(x)). \end{aligned} \quad (32)$$

To satisfy the above condition, solving for a  $\beta \geq 1$  is sufficient. From Equations (31) and (32), it implies that:

$$\alpha \geq \frac{L_\ell}{l_\ell(1 - \lambda)} = \bar{\alpha}_1 \geq 1. \quad (33)$$

Now, the function  $\alpha V(x)$  satisfies all the sufficient conditions stated by Mayne et al. (2000) for the stability of an MPC under the terminal constraint  $\hat{x}(N) \in \mathbb{X}_s$  which is equivalent to  $V(\hat{x}(N)) \leq l_s$ , without discount (with  $\gamma = 1$ ).

Since we do not wish to have such a terminal constraint, we wish for another lower bound  $\hat{\alpha}_2 \geq 1$  such that, if  $\alpha \geq \bar{\alpha}_2$ , then  $V(\hat{x}(N)) \leq l_s$  at the optimal solution. The computation of this  $\bar{\alpha}_2$  has been outlined by Limon et al. (2009) for the undiscounted case. Since our constraints are closed, bounded and they contain the origin, our model and the MPC control law are both Lipschitz, we directly use the result from Limon et al. (2009) to compute  $\bar{\alpha}_2$ :

$$\bar{\alpha}_2 = \frac{\sum_{i=0}^{N-1} \ell(\tilde{x}(i), \tilde{u}(i)) - N d}{(1 - \rho)l_s} \quad (34)$$

where  $\tilde{x}(i), \tilde{u}(i)$  represent a sub-optimal state-action sequence for which  $V(\tilde{x}(N)) \leq \rho l_s$  with  $\rho \in [0, 1)$ , and  $d$  is a lower bound for the stage loss  $\ell$  for all  $x$  outside  $\mathbb{X}_s$  and all  $u$  in  $\mathbb{U}$ .

Then, one can take:

$$\alpha \geq \max(\bar{\alpha}_1, \bar{\alpha}_2) = \bar{\alpha} \quad (35)$$

to guarantee stability when  $\gamma = 1$ .

When the discount factor ( $\gamma < 1$ ) is used, condition (29) is still respected by the same range of  $\alpha$  since

$$\gamma V(x^+) - V(x) \leq V(x^+) - V(x). \quad (36)$$

However, from the discussion in (Gaitsgory et al., 2015), for infinite horizon optimal control, it appears that Equation (29) is not sufficient for  $J_{MPC}^*(x)$  to be a Lyapunov function, even when a terminal constraint is used.

We wish to find a lower-bound  $\bar{\gamma}$  such that, given  $\alpha$  satisfying Equation (35), the MPC is stable for  $\gamma \geq \bar{\gamma}$ . For infinite-horizon optimal control, this was done by Gaitsgory et al. (2015). First, recall that:

$$\begin{aligned}\alpha V(x) &\leq \alpha L_V \|x\|_2^2 \leq \alpha \frac{L_V}{l_\ell} \ell(x, 0) \\ &= C \inf_{u \in \mathbb{U}} \ell(x, u). \quad (37)\end{aligned}$$

In Gaitsgory et al. (2015), it shown that  $1 \leq C < 1/(1 - \gamma)$  is sufficient for stability of an infinite-horizon discounted optimal control problem, when  $\alpha V(x)$  is its value function. This means that:

$$\frac{\alpha L_V}{l_\ell} < \frac{1}{1 - \gamma}, \quad (38)$$

which implies that:

$$\gamma > 1 - \frac{l_\ell}{\alpha L_V} = \bar{\gamma}_1 \in [0, 1). \quad (39)$$

For MPC, we will instead present an additional condition to the above one that leads to at least convergence to the safe set. This results in a bounded and safe solution. Exact convergence to the origin will be then confirmed when  $V$  is the actual value function, as in Gaitsgory et al. (2015), or if we switch to the demonstrating policy,  $K_0$ , once in the terminal set. Finally, we will remove the terminal constraint as done for the undiscounted case with a final bound on  $\alpha$  and  $\gamma$ .

Recall that condition (29) applies. If the terminal constraint was met at time  $t$ , namely, if  $V(x^*(N)) \leq l_s$ , then at the next time step,  $t + 1$  we have that  $u(N + 1) = K_0(x^*(N))$  is feasible. Hence, the optimal MPC solution can be upper-bounded by the shifted solution at the previous time  $t$ , with the  $K_0$  policy appended at the end of the horizon (Mayne et al., 2000). Denote this policy as  $\tilde{u}$  and  $\tilde{x}$  as the predictions. We have that:

$$\begin{aligned}\Delta J_{MPC}^*(x) &= J_{MPC}^*(x^+) - J_{MPC}^*(x) \\ &\leq J_{MPC}(x^+, \tilde{u}) - J_{MPC}^*(x).\end{aligned}$$

Hence,

$$\begin{aligned}\Delta J_{MPC}^*(x) &\leq \sum_{i=1}^N \gamma^{i-1} \ell(\tilde{x}(i), \tilde{u}(i)) + \gamma^N \alpha V(\tilde{x}^+(N)) \\ &\quad - \ell(x, \tilde{u}(0)) - \sum_{i=1}^{N-1} \gamma^i \ell(\tilde{x}(i), \tilde{u}(i)) \\ &\quad - \gamma^N \alpha V(\tilde{x}(N)) \\ &= (1 - \gamma) L_{N-1}(x) - \ell(x, \tilde{u}(0)) \\ &\quad + \gamma^N (\alpha V(\tilde{x}^+(N)) - \alpha V(\tilde{x}(N))) \\ &\quad + \ell(\tilde{x}(N), K_0(x)) \\ &\leq (1 - \gamma) L_{N-1}(x) - \ell(x, \tilde{u}(0)),\end{aligned}$$

where  $L_{N-1}(x) = \sum_{i=1}^{N-1} \gamma^{i-1} \ell(\tilde{x}(i), \tilde{u}(i))$ .

Now, for  $\gamma = 1$ , the effect of  $L_{N-1}$  disappears and the MPC optimal cost is a Lyapunov function as in the standard MPC stability result from (Mayne et al., 2000). By inspection of  $L_{N-1}$ , since the cost is bounded over bounded sets, also a small enough  $\gamma$  could be found such that  $L_{N-1}(x) < \ell(x, \tilde{u}(0))$ . This  $\gamma$ , however, depends on  $x$ . Consider  $x \notin \mathbb{X}_s$ , for which there exist a feasible solution, namely a solution providing  $\tilde{x}(N) \in \mathbb{X}_s$ . Then, since  $\ell$  is strictly increasing,  $\ell(0, 0) = 0$ ,  $\mathbb{X}_s$  contains the origin and the constraints are bounded, we have that there exist a  $v \geq 1$  such that for any feasible  $x$ :

$$\bar{L}_{N-1} = v(N - 1) \inf_{x \notin \mathbb{X}_s} \ell(x, 0),$$

is an upper bound for  $L_{N-1}(x)$ . For instance,

$$v = \frac{\sup_{(x,u) \in \epsilon \mathbb{X} \times \mathbb{U}} \ell(x, u)}{\inf_{x \notin \mathbb{X}_s} \ell(x, 0)},$$

is sufficient for any closed set of initial conditions  $x(0) \in \epsilon \mathbb{X} \supset \mathbb{X}_s$ , with  $\epsilon > 0$ . In order to have stability, it suffices to have  $(1 - \gamma) \bar{L}_{N-1} - \ell(x, \tilde{u}(0)) \leq 0$  which requires:

$$\gamma \geq 1 - \frac{\ell(x, \tilde{u}(0))}{\bar{L}_{N-1}} = \bar{\gamma}(x). \quad (40)$$

In the above condition  $\bar{\gamma}(x)$  can be less than 1 only outside a neighborhood of origin. Consider again

$$d = \inf_{x \notin \mathbb{X}_s} \ell(x, 0). \quad (41)$$

Then taking

$$\gamma \geq 1 - \frac{d}{\bar{L}_{N-1}} = \bar{\gamma}_2 \in (0, 1), \quad (42)$$

provides that the system trajectory will enter the safe set  $\mathbb{X}_s$ , hence  $\mathbb{B}_\gamma \subseteq \mathbb{X}_s$ . Finally, once  $x \in \mathbb{X}_s$ , we that the policy  $K_0(x)$  is feasible and:

$$\ell(x, K_0(x)) \leq \alpha V(x) - \alpha V(x^+) \leq \alpha V(x).$$



Hence, we can use this policy to upper bound the MPC cost:

$$J_{MPC}^*(x) \leq \sum_{i=0}^{N-1} \gamma^i \alpha V(\tilde{x}(i)) + \gamma^N \alpha V(\tilde{x}(N)).$$

If the above is true with equality, then we can proceed as in Theorem 3.1 of Gaitsgory et al. (2015), with  $\gamma > \bar{\gamma}_1$ . This would require  $\alpha V(x)$  to be also a value function for the discounted problem.

From the above considerations, we can conclude that that:

1. If  $N = 1$ , then  $\bar{L}_{N-1} = 0$  and the system is asymptotically stable for any  $\gamma > 0$ .
2. If  $N > 1$ ,  $\gamma \geq \bar{\gamma}_2$ , then the system reaches an bound  $\mathbb{B}_\gamma$  that is included in  $\mathbb{X}_s$ .
3. If  $N > 1$   $\gamma \geq \bar{\gamma}_2$  and once in  $\mathbb{X}_s$  we switch to the policy  $K_0(x)$  then the system is asymptotically stable.
4. If  $\alpha V(x)$  is the global value function for the discounted problem and if  $\mathcal{R}(\mathbb{X}_s) = \mathbb{X}_s$ , then  $\gamma > \bar{\gamma}_1$  provides that the system is Asymptotically stable.
5. If  $\alpha V(x)$  is only the value function in  $\mathbb{X}_s$  for the discounted problem, and if  $\mathcal{R}(\mathbb{X}_s) \neq \mathbb{X}_s$ , then  $\gamma > \max(\bar{\gamma}_1, \bar{\gamma}_2)$  provides that the system is Asymptotically stable.

Finally, following Theorem 3 from (Limon et al., 2003), the terminal constraint can be removed for all points  $x \in \mathcal{R}^N(\rho\mathbb{X}_s)$ , with  $\rho \in [0, 1)$ , by setting:

$$\alpha \geq \bar{\alpha} = \max(\bar{\alpha}_1, \bar{\alpha}_3), \quad (43)$$

$$\bar{\alpha}_3 = \frac{\bar{L}_N - \frac{1-\gamma^N}{1-\gamma} d}{(1-\rho)\gamma^N l_s} > 0. \quad (44)$$

In fact, by the same argument of Limon et al. (2003), for any states for which it exists a feasible sequence  $\tilde{u}$  taking  $\hat{x}(N)$  to  $\rho\mathbb{X}_s$  we have that:

$$J_{MPC}^*(x) \leq J_{MPC}(x, \tilde{u}) = L_N(x) + \rho \alpha \gamma^N l_s. \quad (45)$$

If  $\alpha$  satisfies (43), then we also have that:

$$(1-\rho)\alpha \gamma^N l_s \geq L_N(x) - \frac{1-\gamma^N}{1-\gamma} d, \quad (46)$$

from which we can directly verify that the set defined in (16) is a ROA (for either asymptotic or practical stability):

$$\Upsilon_{N,\gamma,\alpha} = \left\{ x \in \mathbb{R}^{n_x} : J_{MPC}^*(x) \leq \frac{1-\gamma^N}{1-\gamma} d + \gamma^N \alpha l_s \right\}.$$

**Robustness** For point 6, the stability margins of nominal MPC have been studied in (Limon et al., 2009). In particular, in a setup without terminal constraint, under nominal stabilising conditions, with a uniformly continuous model (in our case even Lipschitz), cost functions being also uniformly continuous, then the optimal MPC cost is also uniformly continuous (Limon et al., 2009, Proposition 1). In other words, from (Limon et al., 2009, Lemma 1), there is a  $\mathcal{K}_\infty$ -function,  $\sigma$ , such that at the optimal solution,  $\underline{u}^*$ , we have:

$$|J_{MPC}^*(x+w) - J_{MPC}^*(x)| \leq \sigma(\|w\|). \quad (47)$$

Using the above identity, one wish to bound the increase in the MPC cost due to uncertainty. At the same time, we wish the MPC to remain feasible and perform a contraction, namely, to have a stability margin. Since we are using soft constraints, then the MPC remains always feasible, however, we need the predictions at the end of the horizon to be in an invariant set  $\mathbb{X}_s$  even under the effect of uncertainty. In particular, we will use  $V(x)$  and its contraction factor  $\lambda$  to compute a smaller level set  $\zeta\mathbb{X}_s$ , for some  $\zeta \in (0, 1)$  which is invariant under the uncertainty. Once this is found then we can compute a new  $\alpha$  for this set according to (43). In particular, under the policy  $K_0$ , we have that:

$$\begin{aligned} V(x^+ + w) - V(x) &\leq V(x^+) - V(x) + L_V \|w\|_2^2 \\ &\leq (\lambda - 1)V(x) + L_V \|w\|_2^2. \end{aligned}$$

We wish this quantity to be non-positive for  $x \notin \zeta\mathbb{X}_s$ , which means that  $V(x) \geq \zeta l_s$ . For this it is sufficient to have:

$$\|w\|_2^2 \leq \bar{\mu}^2 = \frac{1-\lambda}{L_V} \zeta l_s \leq \frac{1-\lambda}{L_V} V(x) \quad (48)$$

Therefore, given the model error  $w$ , if the MPC remains feasible and if  $\alpha$  and  $\gamma$  exceed their lower bounds given the restricted set  $\zeta\mathbb{X}_s$ , we have that  $\|w\|_2 \leq \bar{\mu}$  implies that:

$$\begin{aligned} \Delta J_{MPC}^*(x) &= J_{MPC}^*(x^+ + w) - J_{MPC}^*(x) \\ &\quad + J_{MPC}^*(x^+) - J_{MPC}^*(x^+) \\ &\leq J_{MPC}(x^+, \tilde{u}) - J_{MPC}^*(x) + \sigma(\|w\|) \\ &\leq (1-\gamma)\bar{L}_{N-1} - \ell(x, \tilde{u}(0)) + \sigma(\|w\|) \\ &\leq -l_\ell \|x\|_2^2 + \sigma(\|w\|) + \bar{d}(N), \end{aligned}$$

which is the definition of Input-to-State practical Stability (Khalil, 2014; Limon et al., 2009), where we have defined  $\bar{d}(N) = (1-\gamma)\bar{L}_{N-1}$ . The trajectory of the system is therefore bounded by the level-set of  $J_{MPC}^*(x)$  outside which  $\sigma(\mu) + \bar{d}(N) \leq l_\ell \|x\|_2^2$ . Since  $\sigma$  is strictly increasing and  $\bar{d}$  is strictly decreasing, we can also conclude that the size of this bound increases with increasing model error  $\mu$  and with the horizon length  $N$ . Note that the term  $\bar{d}$  vanishes if  $\gamma = 1$  but the term  $\sigma$  will also increase with  $N$  if  $\bar{L}_f > 1$ . From the restriction of the terminal set, it also

follows that the ROA defined in Equation (16) will also be restricted unless we recompute a larger  $\alpha$  for this new set.  $\square$

In practice, the ISS bound  $\sigma(\mu)$  from Lemma 1 has a form similar to the one discussed for the constraint penalty in the proof of Lemma 2, see Equation (28). Its explicit computation is omitted for brevity; however, in general, we can expect the bound to become worse for systems that are open-loop unstable as the horizon length increases.

## B. MPC as SQP Formulation

We solve the MPC problem through iterative linearisations of the forward model, which gives the state and input matrices:

$$A(i) = \left. \frac{\partial \hat{f}}{\partial x} \right|_{\bar{x}(i)}, \quad B(i) = \left. \frac{\partial \hat{f}}{\partial u} \right|_{\bar{u}(i)}. \quad (49)$$

These are evaluated around a reference trajectory:

$$\bar{x}^* = \{\bar{x}^*(i), i = 0, \dots, N\}, \quad (50)$$

$$\bar{u}^* = \{\bar{u}^*(i), i = 0, \dots, N-1\}. \quad (51)$$

This is initialised by running the forward model with zero inputs, and then updated at each iteration by simulating the forward model on the current optimal solution.

The Lyapunov function  $V$  is expanded to a second order term by using Taylor expansion and is evaluated around the same trajectory. The Jacobian and Hessian matrices, respectively,  $\Gamma$  and  $H$ , are:

$$\Gamma = \left. \frac{\partial V}{\partial x} \right|_{\bar{x}(N)}, \quad H = \frac{1}{2} \left. \frac{\partial^2 V}{\partial^2 x} \right|_{\bar{x}(N)}. \quad (52)$$

All the quantities in Equation (49) and (52) are computed using automatic differentiation. Using these matrices, we solve the convex optimization problem:

$$\begin{aligned} \delta \underline{u}^* = \arg \min \quad & \gamma^N \alpha \left( \|H^{1/2} \delta \hat{x}(N)\|_2^2 + \Gamma^T \delta \hat{x}(N) \right) \\ & + \sum_{i=0}^{N-1} \gamma^i \ell(\hat{x}(i), \hat{u}(i)) \end{aligned} \quad (53)$$

$$\begin{aligned} \text{s.t. } \quad & \hat{x}(i+1) = A(i)\delta \hat{x}(i) + B(i)\delta \hat{u}(i) + \hat{f}(\bar{x}(i)), \\ & \hat{x}(i) - \delta \hat{x}(i) = \bar{x}(i) \\ & \hat{u}(i) - \delta \hat{u}(i) = \bar{u}(i) \\ & \hat{x}(i) \in \mathbb{X}, \forall i \in [0, N], \\ & \hat{u}(i) \in \mathbb{U}, \forall i \in [0, N-1], \\ & \hat{x}(0) = x(t), \\ & \|\delta \hat{u}(i)\|_\infty \leq r_{\text{trust}}, \forall i \in [0, N-1], \end{aligned}$$

where the state constraints are again softened and the last inequality constraint is used to impose a trust region with a fixed radius,  $r_{\text{trust}}$ . This notably improves the search for an optimal solution, as shown for the inverted pendulum case in Figure 15.

Once problem (53) is solved, we obtain the delta sequence  $\delta \underline{u}^*$ . The new optimal solution is then computed according to the update rule:

$$\underline{u}^* \leftarrow \underline{u}^* + lr \delta \underline{u}^*,$$

where  $lr < 1$  is a learning rate, which is annealed after each iteration. Finally, the reference trajectories used for the next linearisation are  $\underline{u}^*$  and the state series resulting from simulating the forward model on  $\underline{u}^*$ , namely

$$\bar{x}^* = \hat{f} \circ \underline{u}^*.$$

This is summarised in Algorithm 2. Interested readers can find more details on SQP in the work by Nocedal & Wright (2006); Hadfield-Menell et al. (2016), where adaptive schemes for computing the trust radius are discussed.

---

### Algorithm 2 Neural Lyapunov MPC solver

---

**In:**  $x(t), \hat{f}, \alpha, V, N_{\text{steps}}, \epsilon_{lr} \in [0, 1], r_{\text{trust}} > 0, lr$

**Out:**  $u(t)$

---

```

 $\bar{x}^* \leftarrow \{x(t)\}^{N+1}, \quad \underline{u}^* \leftarrow \{0\}^N$ 
for  $j = 0, \dots, N_{\text{steps}}$  do
     $\{A(i)\}, \{B(i)\} \leftarrow$  linearisation of  $\hat{f}$  using Equation (49)
     $(\Gamma, H) \leftarrow$  Taylor expansion of  $V$  using Equation (52)
     $\delta \underline{u}^* \leftarrow$  solution of optimization problem (53)
     $\underline{u}^* \leftarrow \underline{u}^* + lr \delta \underline{u}^*$ 
     $\bar{x}^* \leftarrow \hat{f} \circ \underline{u}^*$ 
     $lr \leftarrow (1 - \epsilon_{lr}) lr$ 
 $u(t) \leftarrow \underline{u}^*(0)$ 
    
```

---

## C. Experimental Setup

We demonstrate our approach on an inverted pendulum and a vehicle kinematics control problem. We implement our code using PyTorch (Paszke et al., 2019).

### C.1. Implementation Specifics

A practical consideration for implementing Algorithm 1 is tuning the MPC terminal cost scaling,  $\alpha$ , via grid-search. The MPC needs to run over the entire dataset of initial points,  $\mathcal{X}_0 = \{x_m(0)\}_{m=1}^M$ , with different configurations. In order to speed up the search for  $\alpha$ , we run the MPC only on a sample of 20% of the initial dataset. Once the optimal  $\alpha$  is found, only then we run the MPC over the entire dataset and use this data to compute the next  $V(x)$ .

Additionally to what presented in the main text, we param-

Table 4: **Configuration for Experiments.** We specify the parameters used for the simulation of the system dynamics, the MPC demonstrator, the Neural Lyapunov MPC as well as for the alternate learning algorithm.

PARAMETER	SYMBOL	VALUE	
		CAR KINEMATICS	PENDULUM
GENERAL			
MASS	$m$	-	0.15 kg
LENGTH	$l$	-	0.5 m
ROTATIONAL FRICTION	$\lambda_F$	-	0.1 N m s rad <sup>-1</sup>
GRAVITY	$g$	-	9.81 m s <sup>-2</sup>
SAMPLING TIME	$dt$	0.2 s	0.01 s
STATE CONSTRAINT	$\mathbb{X}$	$[-1, 1]^2 \times [-\pi, \pi]$	$[-\pi, \pi] \times [-2\pi, 2\pi]$
INPUT CONSTRAINT	$\mathbb{U}$	$[-10, 10] \times [-2\pi, 2\pi]$	$[-0.64, 0.64]$
STATE PENALTY	$Q$	DIAG(1, 1, 0.001 $\pi$ )	DIAG(0.1, 0.1)
INPUT PENALTY	$R$	DIAG(100, 20 $\pi$ )	0.1
DISCOUNT FACTOR	$\gamma$	1	1
DEMONSTRATOR MPC			
HORIZON	$N$	5	5
# OF LINEARISATIONS	$N_{steps}$	3	10
TRUST REGION	$r_{trust}$	$\infty$	2.5
LEARNING RATE	$lr$	0.9	0.9
DECAY RATE	$\epsilon_{lr}$	0.2	0.2
TERMINAL PENALTY	$P$	400 $Q$	500 $P_{\text{LQR}}$
NEURAL LYAPUNOV MPC			
HORIZON	$N$	1	1
# OF LINEARISATIONS	$N_{steps}$	18	18
TRUST REGION	$r_{trust}$	0.005	0.5
LEARNING RATE	$lr$	0.9	0.9
SCALING OF $V$	$\alpha$	TABLE 6	TABLE 8
DECAY RATE	$\epsilon_{lr}$	0.02	0.02
$V_{net}$ ARCHITECTURE	MLP	(128, 128, 128)	(64, 64, 64)
$V_{net}$ OUTPUT	$n_V \times n_x$	400 $\times$ 3	100 $\times$ 2
ALTERNATE LEARNING			
OUTER ITERATIONS	$N_{ext}$	3	2
ENLARGEMENT FACTOR	$\epsilon_{ext}$	0.1	0.1
MPC LINE SEARCH	$\alpha_{list}$	{1, 6, ..., 36}	{0.2, 0.4, ..., 2}
LYAPUNOV EPOCHS	$N_V$	500	200
LOSS EQUATION (9)	$\rho$	0.0001	0.0001
LQR DECREASE FACTOR	$v$	0	1
CONTRACTION FACTOR	$\lambda$	0.99	0.99
LYAPUNOV LEARNING RATE	$lr$	0.001	0.001
LYAPUNOV WEIGHT DECAY	$wd$	0	0.002

terize  $V(x)$  with a trainable scaling factor,  $\beta$ , as:

$$V(x) = \text{softplus}(\beta)x^T (\ell_\ell I + V_{net}(x)^T V_{net}(x)) x, \quad (54)$$

where  $\text{softplus}(x) = \log(1 + \exp(x))$ . The parameter  $\beta$  is initialized to 1 in all experiments except for the inverted pendulum without LQR loss, i.e. for results in Figure 14.

The full set of parameters for the experiments can be found in Table 4.

## C.2. Baseline Controllers

Our Neural Lyapunov MPC has a single-step horizon and uses the learned Lyapunov function as the terminal cost. To compare its performance, we consider two other MPCs:

- **Long-horizon MPC (demonstrator):** An MPC with a longer horizon and a quadratic terminal cost  $x^T P x$ . This MPC is also used to generate the initial demonstrations for alternate learning.
- **Short-horizon MPC:** An MPC with a single-step horizon and the same terminal cost as the long-horizon MPC. All other parameters are the same as the Neural Lyapunov MPC except  $\alpha$ , which is tuned manually.

## C.3. Forward models

We use an Euler forward model for the environments. Consider  $dt$  as the sampling time, then the state transition is:

$$\eta(t+1) = \eta(t) + dt f_u(\eta(t), u(t)), \quad (55)$$

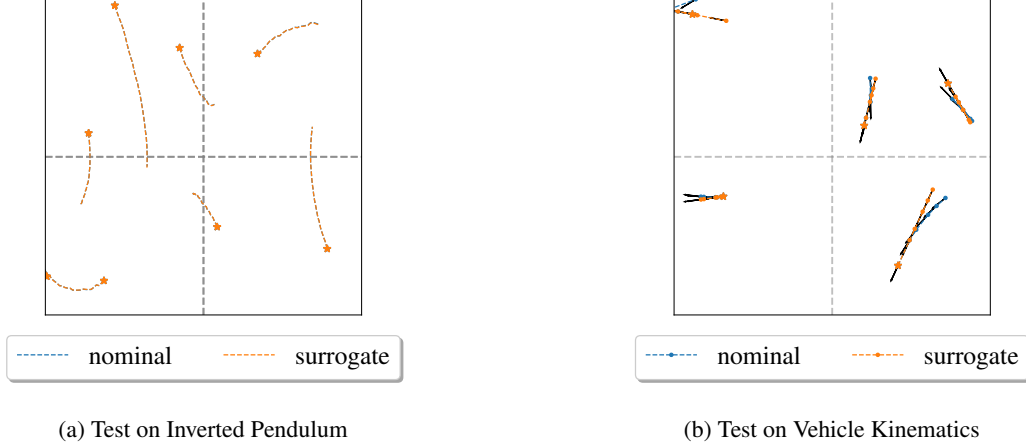


**Figure 6: Testing the surrogate models.** We generate each trajectory by propagating an initial state  $\eta(0)$  with input sequence  $\{u(t)\}_{t=0}^{T-1}$  through the nominal system and the learned surrogate model. (a) For the inverted pendulum:  $u(t) \sim \mathcal{U}([-0.4, 0.4])$  and simulation is performed for  $T = 25$ . (b) For the vehicle kinematics:  $u(t) \sim \mathcal{U}([-0.1, 0.1] \times [-0.1, 0.1])$  and simulation is performed for  $T = 5$ .

where  $\eta(t)$  is the state,  $u(t)$  is the input and  $f_u(\eta(t), u(t))$  is the time-invariant, deterministic dynamical system.

#### C.3.1. VEHICLE KINEMATICS

**World model** For the non-holonomic vehicle,  $\eta = (x, y, \phi) \in \mathbb{R}^3$  is the state, respectively, the coordinates in the plane and the vehicle orientation, and  $u = (v, \omega) \in \mathbb{R}^2$  is the control input, respectively, the linear and angular velocity in the body frame.  $f_u(\eta, u)$  encodes the coordinate transformation from the body to the world frame (Fossen, 2011):

$$f_u(\eta(t), u(t)) = \begin{pmatrix} \dot{x} \\ \dot{y} \\ \dot{\phi} \end{pmatrix} = \begin{pmatrix} v(t) \cos \phi(t) \\ v(t) \sin \phi(t) \\ \omega(t) \end{pmatrix} \quad (56)$$

$$= \underbrace{\begin{pmatrix} \cos \phi(t) & 0 \\ \sin \phi(t) & 0 \\ 0 & 1 \end{pmatrix}}_{J(\eta)} \begin{pmatrix} v(t) \\ \omega(t) \end{pmatrix}$$

**Surrogate model** We build a gray-box model using a neural network to model  $J(\eta)$ , similar to the work by Quaglino et al. (2020). The input feature to the network is  $\sin \phi$  and  $\cos \phi$ , where  $\phi$  is the vehicle’s orientation. The network consists of a hidden layer with 20 hidden units and tanh activation function, and an output layer without any activation function. The weights in the network are initialized using Xavier initialization (Glorot & Bengio, 2010) and biases are initialized from a standard normal distribution.

**Training the surrogate model** We generate a dataset of 10K sequences, each of length  $T = 1$ . For each sequence,

the initial state  $\eta(0)$  is sampled uniformly from  $\mathbb{X}$ , while the input  $u(0)$  is sampled uniformly from  $\mathbb{U}$ . We use a training and validation split of 7 : 3. Training is performed for 300 epochs using the Adam optimizer (Kingma & Ba, 2014) and the mean-squared error (MSE) loss over the predicted states. The learning rate is 0.01 and the batch size is 700.

#### C.3.2. INVERTED PENDULUM

**World model** Inverted pendulum is one of the most standard non-linear systems for testing control methods. We consider the following model (Berkenkamp et al., 2017):

$$ml^2 \ddot{\theta} = mgl \sin \theta - \lambda_F \dot{\theta} + u \quad (57)$$

where  $\theta \in \mathbb{R}$  is the angle,  $m$  and  $l$  are the mass and pole length, respectively,  $g$  is gravitational acceleration,  $\lambda_F$  is the rotational friction coefficient and  $u \in \mathbb{R}$  is the control input. We denote the state of the system as  $\eta = (\theta, \dot{\theta}) \in \mathbb{X} \subset \mathbb{R}^2$  and input as  $u \in \mathbb{U} \subset \mathbb{R}$ . We use an Euler discretization, as in Equation (55), to solve the initial-value problem (IVP) associated with the following equation:

$$f_u(\eta(t), u(t)) = \begin{pmatrix} \dot{\theta} \\ \ddot{\theta} \end{pmatrix} = \begin{pmatrix} \dot{\theta}(t) \\ \frac{mgl \sin \theta(t) + u(t) - \lambda_F \dot{\theta}(t)}{ml^2} \end{pmatrix} \quad (58)$$

**Surrogate model** We use a neural network to predict the acceleration of the pendulum,  $\ddot{\theta}(t)$ . The input to the network is the state  $\eta(t)$  and action  $u(t)$  at the current time-step  $t$ . The network is a three layer feedforward network with 64 hidden units and tanh activation in each hidden layer. The output layer is linear. All the layers have no biases and their weights are initialized as in Glorot & Bengio (2010).

**Training the surrogate model** To train the surrogate model, we generate a dataset of  $10K$  sequences, each of length  $T = 1$ . We use MSE loss and Adam optimizer (Kingma & Ba, 2014) to train the model. The rest of the parameters are kept the same as those used for the vehicle kinematics model training.

## D. Additional Results

Here we provide additional results and plots related to the experiments specified in the paper.

### D.1. Vehicle Kinematics

The vehicle model results are run over different machines. The resulting losses and  $\alpha$  are discussed. In all experiments, the parameters of  $V$  are reinitialised after every outer epoch. The Lyapunov loss does not make use of the LQR loss  $\ell$ .

**Choosing number of outer iterations  $N_{ext}$**  We run our algorithm for more iterations on a machine with different operating system. This leads to a slight difference from the results mentioned in the paper. As observed from Table 5, the third iteration leads to the best performance in terms of verified and not verified percentages. We set  $N_{ext} = 3$  in all experiments.

Table 5: **Car Kinematics: Choosing number of outer iterations.** Lyapunov Function learning performed on a different machine (results are slightly different from the ones in the paper).

ITER.	LOSS ( $\log(1+x)$ )	VERIFIED (%)	NOT VERIFIED (%)
1	1.42	92.83	3.95
2	0.91	93.08	4.71
3	0.62	94.26	3.89
4	0.46	93.65	4.38
5	0.53	92.18	5.63

**Alternate learning on nominal model** We train the Neural Lyapunov MPC while using a nominal model for internal dynamics. In Figure 7, we plot the training curves, the resulting Lyapunov function, and line-search for MPC in each outer epoch. The results are also shown in Table 6. As can be seen, tuning the MPC parameter  $\alpha$  helps in minimizing the loss (9) further. Points near the origin don't always verify. The MPC obtained after the third iteration achieves the best performance. This can further be validated from Figure 8, where we plot trajectories obtained by using the Neural Lyapunov MPC from each iteration.

**Alternate learning on surrogate model** In order to test the transfer capability of the approach, we perform the training of Neural Lyapunov MPC using an inaccurate surrogate

model for the internal dynamics. This model is also used for calculating the Lyapunov loss (9) and evaluating the performance of the Lyapunov function. We plot the training curves, the resulting Lyapunov function, and line-search for MPC in each outer epoch in Figure 9. The results of the training procedure are presented in Table 7. The MPC obtained from the second iteration achieves the best performance. In the third iteration, the Lyapunov loss increases and number of verified and not verified points becomes worse. The poor performance also reflects in the trajectories obtained by using the Lyapunov MPC from the third iteration, as shown in Figure 10.

Table 6: **Car Kinematics: Learning on nominal model.** Results for training Neural Lyapunov MPC while using a nominal model for internal dynamics. We use the Lyapunov loss (9) for both learning the Lyapunov function and tuning the MPC. This is specified in the  $\log(1+x)$  scale.

(a) Lyapunov Function Learning			
ITER.	LOSS ( $\log(1+x)$ )	VERIFIED (%)	NOT VERIFIED (%)
1	1.55	92.20	4.42
2	0.87	93.17	4.89
3	0.48	94.87	3.89

(b) MPC Parameter Tuning			
ITER.	LOSS ( $\log(1+x)$ ) BEFORE	LOSS ( $\log(1+x)$ ) AFTER	PARAMETER $\alpha^*$
1	1.55	1.07	26.00
2	0.87	0.71	31.00
3	0.48	0.52	36.00

Table 7: **Car Kinematics: Learning on surrogate model.** Results for training Neural Lyapunov MPC while using the surrogate model for internal dynamics as well as in Lyapunov training. We use the Lyapunov loss (9) for both learning the Lyapunov function and tuning the MPC. This is specified in the  $\log(1+x)$  scale.

(a) Lyapunov Function Learning			
ITER.	LOSS ( $\log(1+x)$ )	VERIFIED (%)	NOT VERIFIED (%)
1	1.84	91.74	8.26
2	1.43	92.26	7.74
3	1.65	91.61	8.39

(b) MPC Parameter Tuning			
ITER.	LOSS ( $\log(1+x)$ ) BEFORE	LOSS ( $\log(1+x)$ ) AFTER	PARAMETER $\alpha^*$
1	1.84	1.41	36.00
2	1.43	1.05	36.00
3	1.65	1.30	36.00

## D.2. Inverted Pendulum

Differently from the car kinematics, for the inverted pendulum task, the parameters of  $V$  are not re-initialized after every outer epoch, and the Lyapunov loss makes use of the LQR loss,  $\ell$ , for all the experiments except for the results in Figure 14. In this section, we discuss the results obtained from the alternate learning on the nominal model. We also provide an ablation study on: 1) a solution based solely on a contraction factor, and 2) the effect of having an imperfect solver, in particular the instability resulting from wrongly tuning the trust-region radius.

**Alternate learning** Since the trained surrogate model has a high accuracy, we only consider the scenario for alternate learning with the nominal model. The main results for this scenario are in Figure 11 and Table 8. We notice a slight improvement in the MPC’s performance in the second iteration of the training procedure. In Figure 11, it can be noticed that a small  $\alpha$  needs to be used, which contradicts the ideal theoretical result. In practice, a very large value of this parameter results in bad conditioning for the QPs used by the MPC and causes the solver to fail.<sup>2</sup> Since the pendulum is open-loop unstable, an increase of the Lyapunov loss can be noticed for larger values of  $\alpha$ . This demonstrates that it is necessary to perform a search over the parameter and that we cannot simply set it to a very large value.

In Figure 12, we show the trajectories obtained by running the Neural Lyapunov MPC obtained from the first and second iterations. The initial states are sampled inside the safe level-set by using rejection sampling. The trajectories obtained from both the iterations are similar even though the Lyapunov function is different. The Lyapunov function from second iteration has a larger ROA.

We also compare the Neural Lyapunov MPC from the second iteration with the baseline MPCs in Figure 13. The baselines controllers behave quite similarly in this problem, although they have different prediction horizons. This is because, for both of them, the LQR terminal cost is a dominating term in the optimization’s objective function. The Neural Lyapunov MPC achieves a slightly slower decrease rate compared to the demonstrator; however, it still stabilizes the system. The transfer from nominal to surrogate model is very successful for all the controllers, though in this case, the surrogate model is particularly accurate.

It should be kept in mind that in order to produce these results, it was necessary to impose in the Lyapunov loss (9) that the decrease rate of  $V(x)$  needs to be upper bounded by the LQR stage loss, as in Equation 5. This resulted in the most effective learning of the function  $V(x)$ , contrarily to the vehicle kinematics example.

Table 8: **Inverted Pendulum: Learning on nominal model.** Results for training Neural Lyapunov MPC while using a nominal model for internal dynamics. We use the Lyapunov loss (9) for both learning the Lyapunov function and tuning the MPC. This is specified in the  $\log(1+x)$  scale.

(a) Lyapunov Function Learning			
ITER.	LOSS ( $\log(1+x)$ )	VERIFIED (%)	NOT VERIFIED (%)
1	3.21	13.25	0.00
2	1.08	13.54	0.00

(b) MPC Parameter Tuning			
ITER.	LOSS ( $\log(1+x)$ ) BEFORE	AFTER	PARAMETER $\alpha^*$
1	3.21	2.47	1.40
2	1.08	1.28	1.00

**Alternate learning without LQR loss** We now consider the case when the learning is performed while using a contraction factor of  $\lambda = 0.9$  and without the LQR loss term in the Lyapunov loss (i.e.,  $v = 0$ ). The results are depicted in Figure 14. In order to obtain these results, the Lyapunov NN scaling  $\beta$ , in Equation (54), was initialized with:

$$\beta_0 = \text{softplus}^{-1}(25),$$

according to a rough estimate of the minimum scaling  $\alpha$  from Equation (33). This was able to produce a Lyapunov function that makes the MPC safe with  $\alpha = 12$ . However, the learning becomes more difficult, and it results in a smaller safe region estimate with a slower convergence rate for the system trajectories.

**Effects of the trust region** In Figure 15, we show the result of varying the trust radius of the SQP solver on the inverted pendulum. While a larger value can result in further approximation, given the limited number of iterations, in this case a small value of the radius results in a weaker control signal and local instability near the origin.

## Acknowledgements

The authors would like to thank Nihat Engin Toklu, Sebastian East, and Mark Cannon for their constructive input, as well as everyone at NNAISENSE, for contributing to an inspiring research environment.

<sup>2</sup>When the solver fails, we simply set the solution to zero.



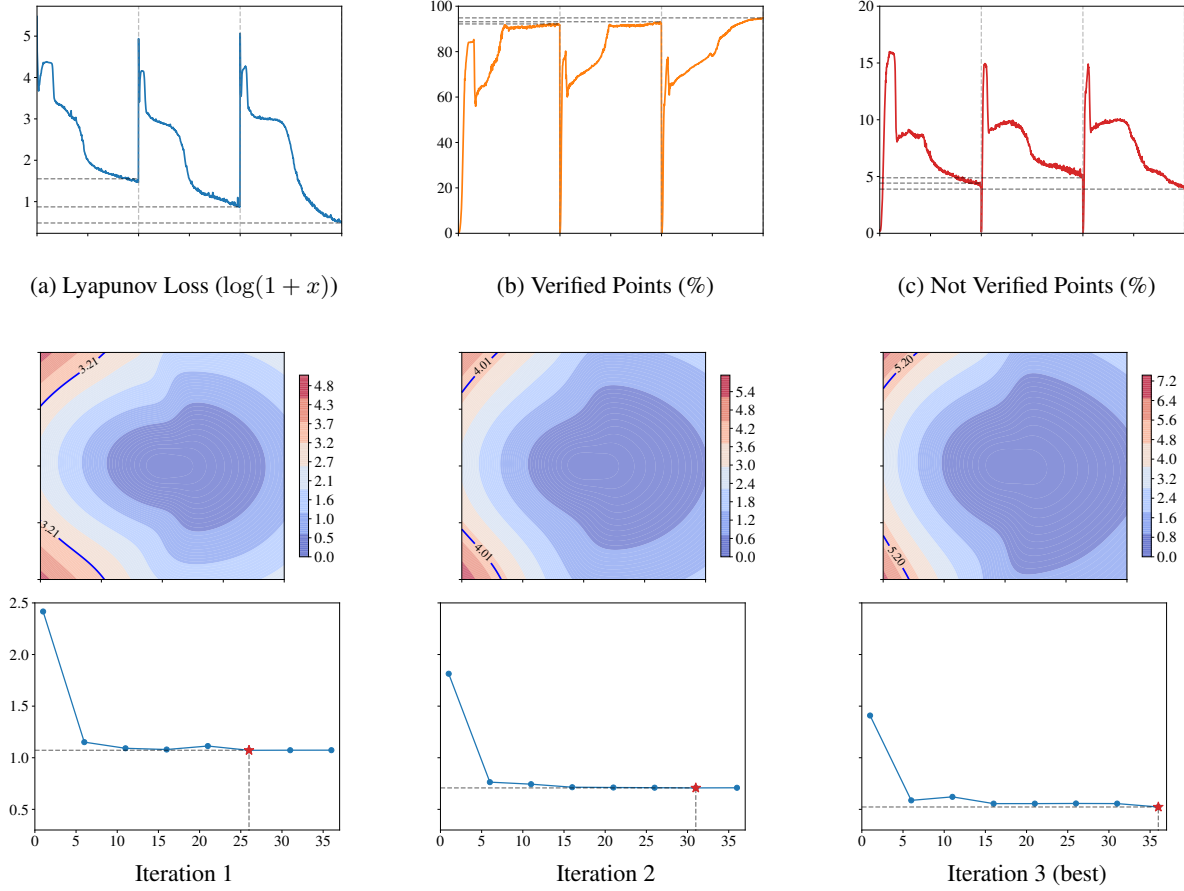


Figure 7: **Car kinematics: Alternate learning on nominal model.** After every  $N_V = 500$  epochs of Lyapunov learning, the learned Lyapunov function is used to tune the MPC parameters. **Top:** The training curves for Lyapunov function. Vertical lines separate iterations. **Middle:** The resulting Lyapunov function  $V$  at  $\phi = 0$  with the best performance. **Bottom:** Line-search for the MPC parameter  $\alpha$  to minimize the Lyapunov loss (9) with  $V$  as terminal cost. The loss is plotted on the y-axis in a  $\log(1+x)$  scale. The point marked in red is the parameter which minimizes the loss.

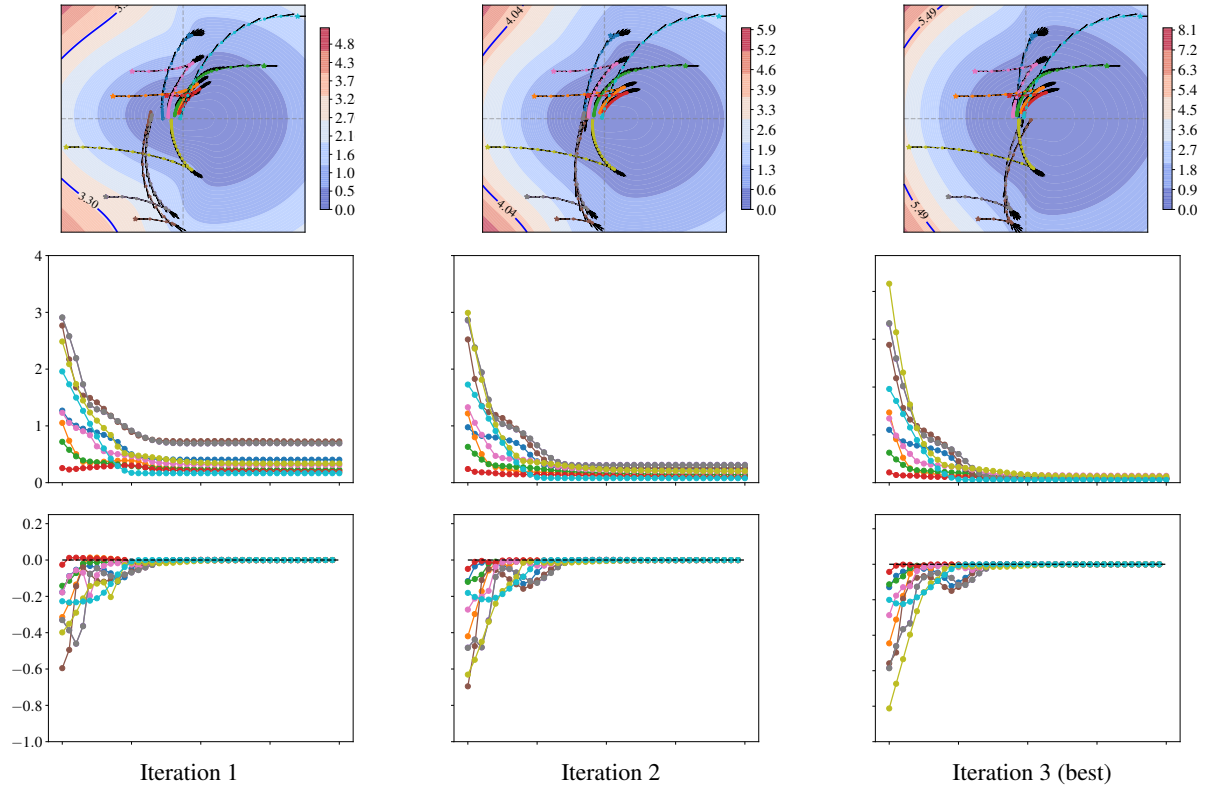


Figure 8: **Car kinematics: Testing Neural Lyapunov MPC obtained from training on nominal model.** For each iteration, we show the trajectories obtained through our Neural Lyapunov MPC while using the resulting Lyapunov function and the MPC parameter selected from the line-search. **Top:** The Lyapunov function at  $\phi = 0$  with trajectories for 40 steps at each iteration. **Middle:** The evaluated Lyapunov function. **Bottom:** The Lyapunov function time difference.

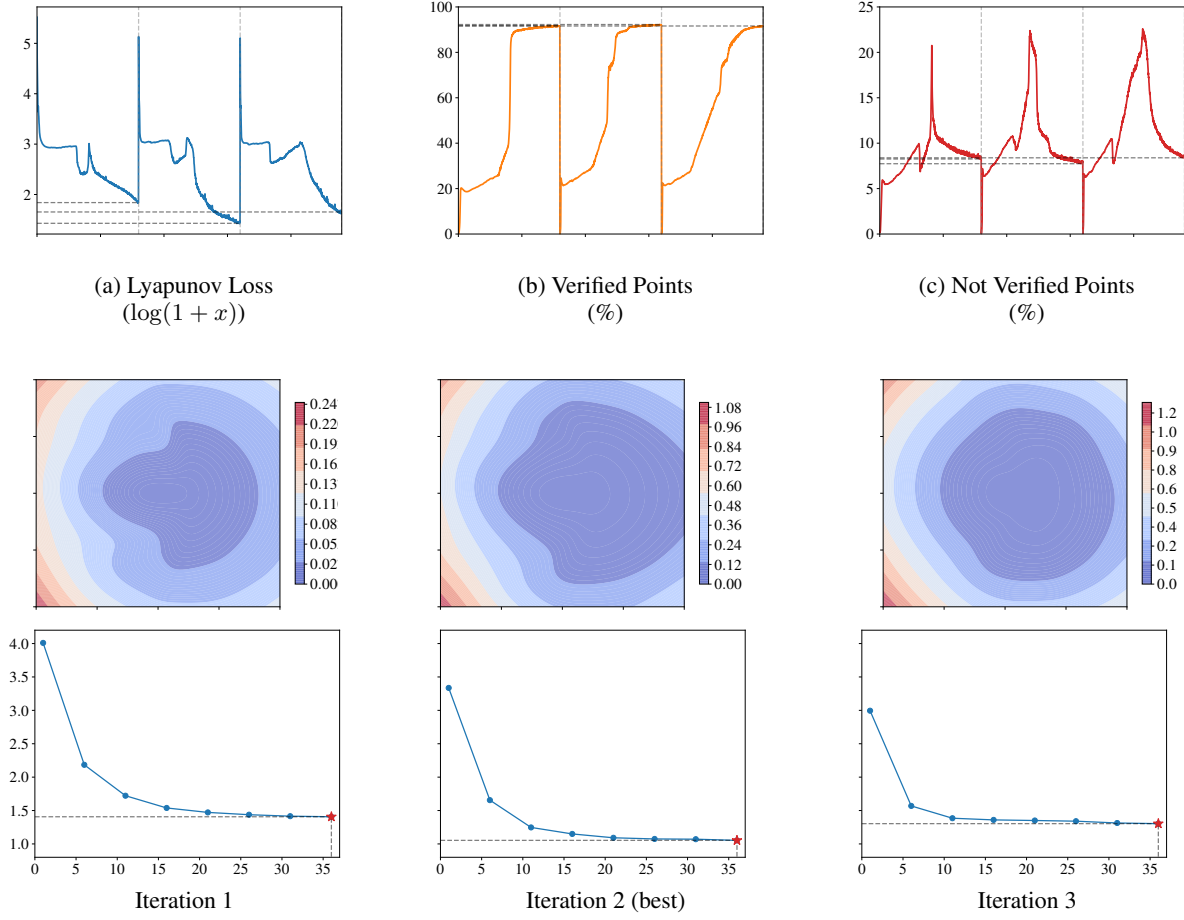


Figure 9: **Car kinematics: Alternate learning on surrogate model.** After every  $N_V = 800$  epochs of Lyapunov learning, the learned Lyapunov function is used to tune the MPC parameters. **Top:** The training curves for Lyapunov function. Vertical lines separate iterations. **Middle:** The resulting Lyapunov function  $V$  at  $\phi = 0$  with the best performance. **Bottom:** Line-search for the MPC parameter  $\alpha$  to minimize the Lyapunov loss (9) with  $V$  as terminal cost. The loss is plotted on the y-axis in a  $\log(1 + x)$  scale. The point marked in red is the parameter which minimizes the loss.

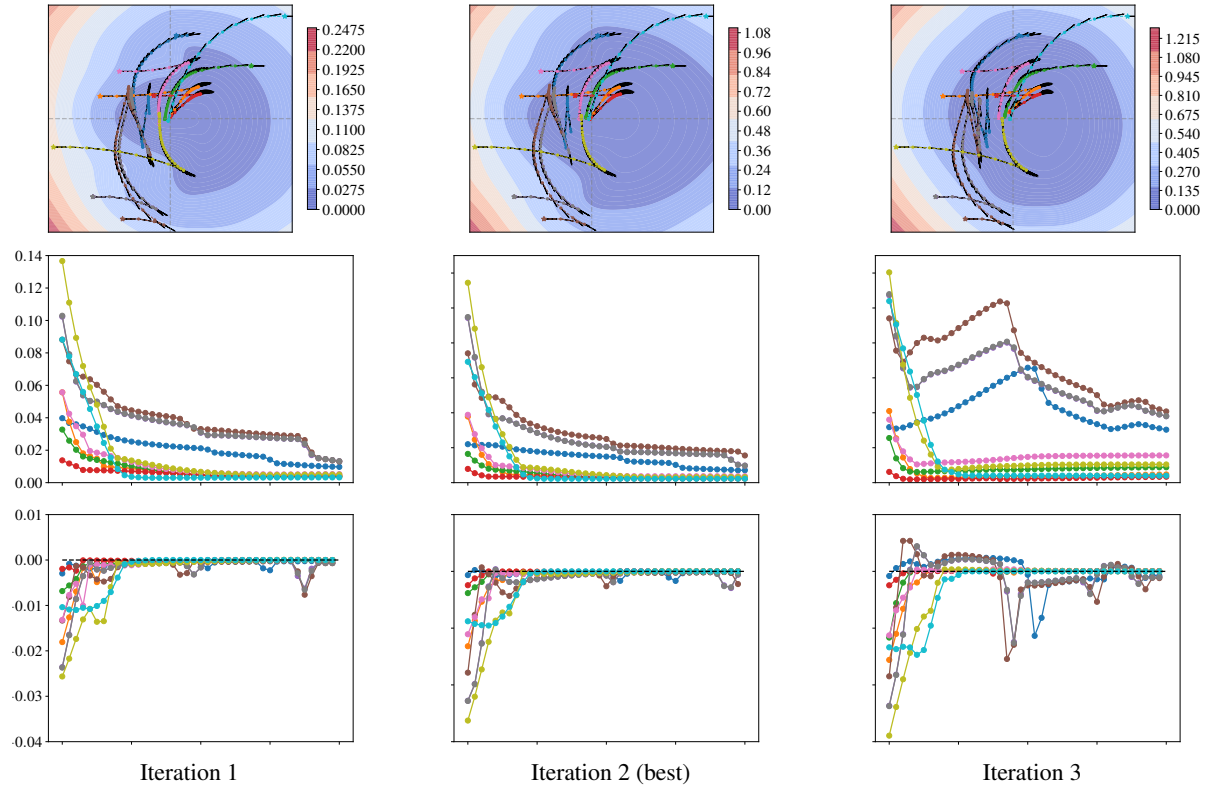


Figure 10: **Car kinematics: Testing Neural Lyapunov MPC obtained from training on surrogate model.** For each iteration, we show the trajectories obtained through our Neural Lyapunov MPC while using the resulting Lyapunov function and the MPC parameter selected from the line-search. **Top:** The Lyapunov function at  $\phi = 0$  with trajectories for 40 steps at each iteration. **Middle:** The evaluated Lyapunov function. **Bottom:** The Lyapunov function time difference.

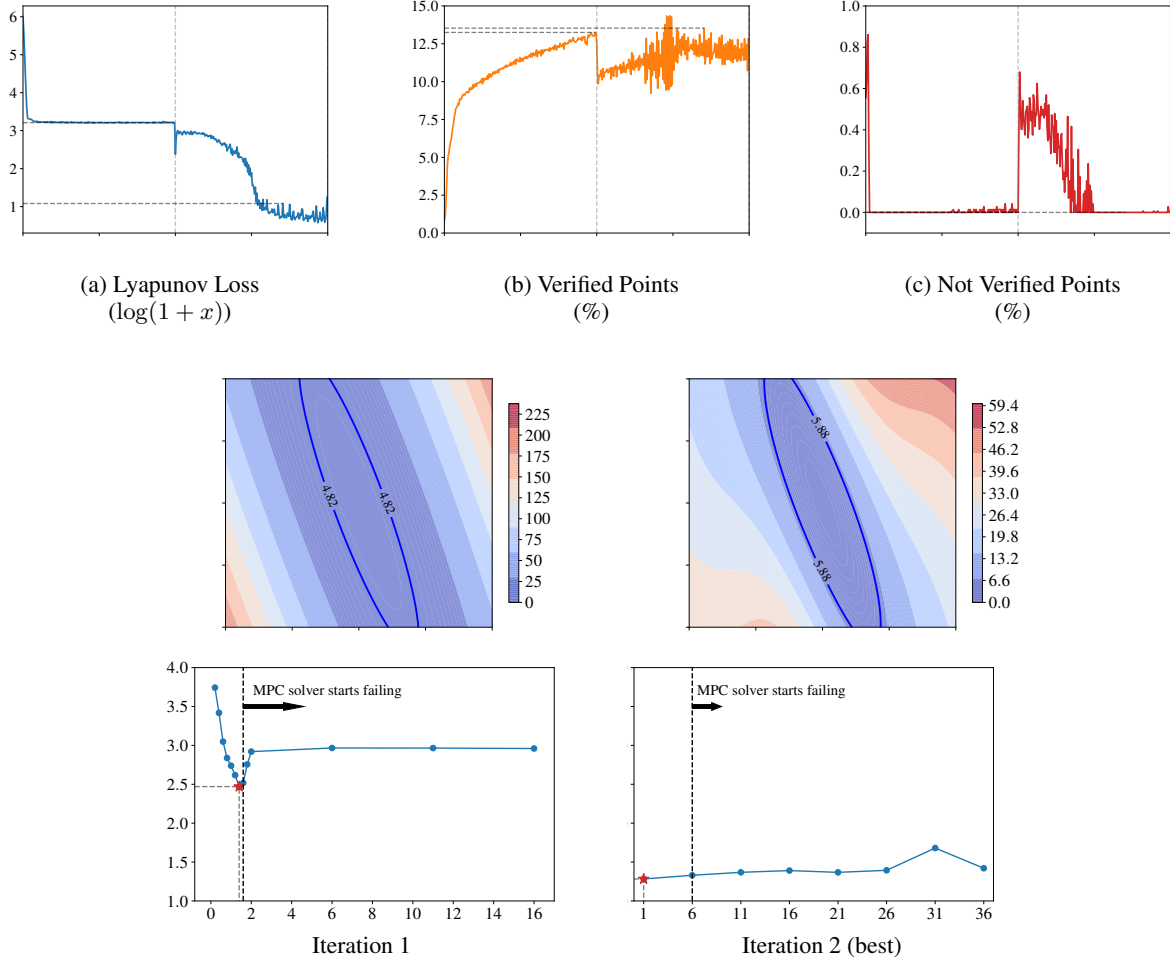


Figure 11: **Inverted Pendulum: Alternate learning on surrogate model.** After every  $N_V = 200$  epochs of Lyapunov learning, the learned Lyapunov function is used to tune the MPC parameters. Unlike the vehicle kinematics example, we do not reinitialize  $V$  between the iterations. **Top:** The training curves for Lyapunov function. Vertical lines separate iterations. **Middle:** The resulting Lyapunov function  $V$  with the best performance. **Bottom:** Line-search for the MPC parameter  $\alpha$  to minimize the Lyapunov loss (9) with  $V$  as terminal cost. The loss is plotted on the y-axis in a  $\log(1+x)$  scale. The point marked in red is the parameter which minimizes the loss.

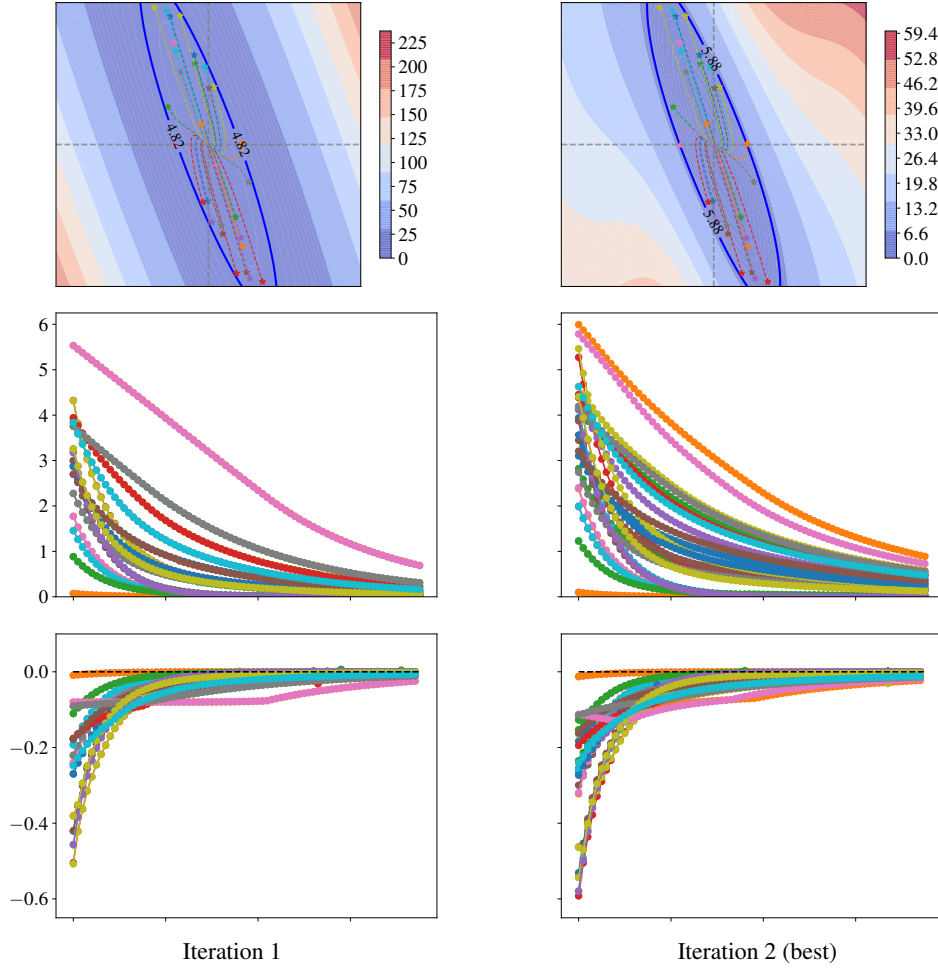


Figure 12: **Inverted Pendulum: Testing Neural Lyapunov MPC obtained from training on nominal model over iterations.** For each iteration, we show the trajectories obtained through our Neural Lyapunov MPC while using the resulting Lyapunov function and the MPC parameter selected from the line-search. The initial states are sampled inside the safe level-set using rejection sampling. **Top:** The Lyapunov function with trajectories for 80 steps at each iteration. **Middle:** The evaluated Lyapunov function. **Bottom:** The Lyapunov function time difference.



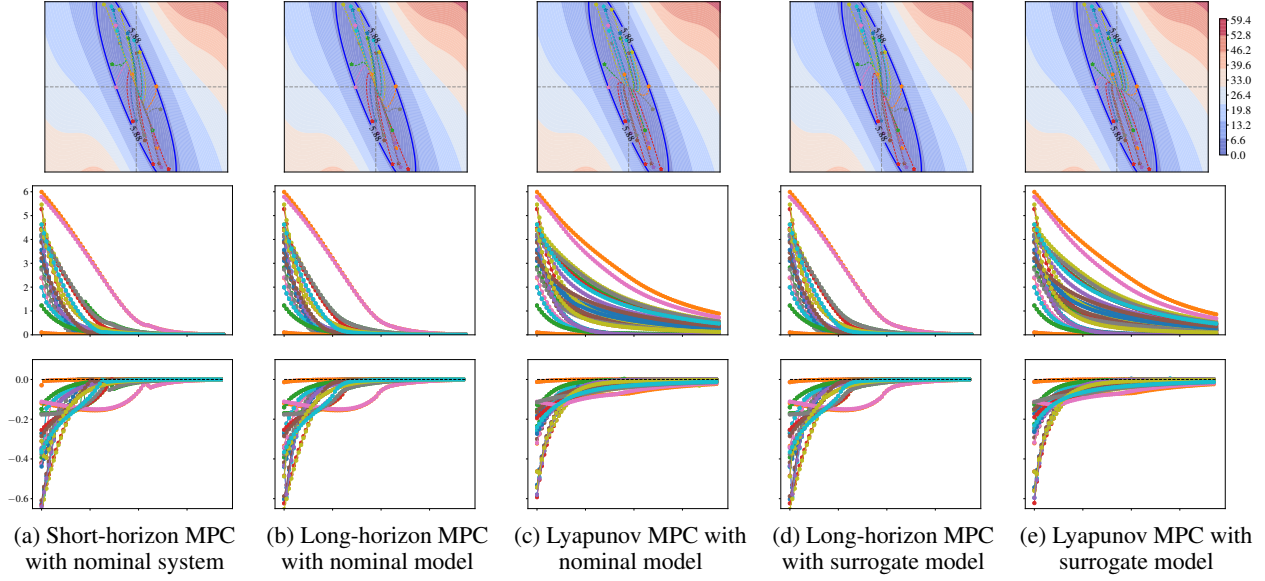


Figure 13: **Inverted Pendulum: Transfer from nominal to surrogate model.** **Top:** The Lyapunov function with overlaid trajectories for 80 timesteps. **Middle:** The Lyapunov function evaluated along trajectories. **Bottom:** The Lyapunov decrease evaluated along trajectories.

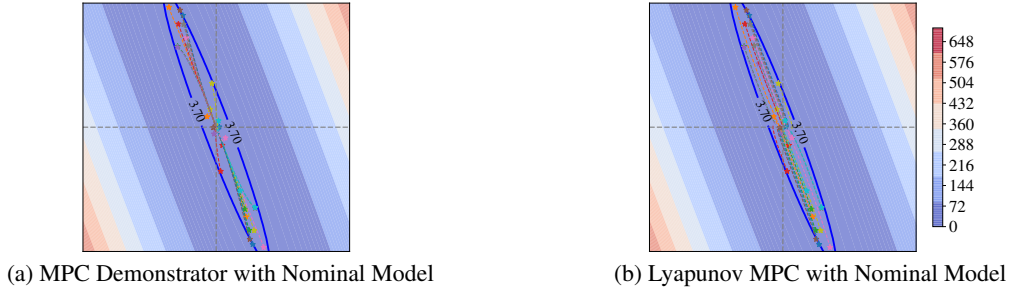


Figure 14: **Inverted Pendulum: Effect of using Lyapunov MPC with contractor factor and no LQR loss.** The Lyapunov function and safe-level set obtained from the first iteration of alternate learning with  $\lambda = 0.9, v = 0$  in the Lyapunov loss (9). This results in a smaller safe region estimate and slower closed-loop trajectories compared to the case when  $\lambda = 0.99, v = 1$ . Each trajectory is simulated for  $T = 80$  timesteps.



Figure 15: **Inverted Pendulum: Effect of trust region on MPC.** The solver hyperparameter,  $r_{\text{trust}}$ , can also affect the stability of the MPC and was tuned manually at this stage. Given the limited amount of solver iterations, a small trust region results in weaker control signals and local instability. A larger trust radius can in this case stabilize the system, while being possibly more sub-optimal. The depicted Lyapunov function is obtained from first iteration of alternate learning and is used by the MPC as its terminal cost.